Chapter 4

Results and Discussion

In this chapter the experimental results of electron interaction with a variety of organic molecules and the discussion of these results are presented. Thereby we go from simple molecules like ethanol to more complex and halogenated (especially fluorinated) compounds. A central point is the investigation of compounds of the structure CF_3COR with variable substituents R bound to the carbonyl group which gives information on the influence of different functional groups on electron induced processes. To demonstrate the influence of a molecular surrounding on specific reaction pathways the experiments were performed in three different states of aggregation (gas phase, molecular clusters and condensed phase). The molecular clusters serve as an intermediate between the isolated molecules and the condensed phase as intermolecular interactions already play an important role but the system is still of limited size and thus more easy to analyze. In the following M will be used for the intact molecule under investigation while $(M\text{-}X)^-$ denotes the formation of an anion due to the loss of an atom or molecule X from the molecule M.

4.1 Ethanol and trifluoroethanol - the influence of fluorination

Dissociative electron attachment to the two alcohols ethanol CH_3CH_2OH and trifluoroethanol CF_3CH_2OH has been studied in order to compare the corresponding fragmentation pathways of these molecules. To get some information on site selectivity the deuterated analogue CF_3CD_2OH was investigated as well. The corresponding molecular structures are depicted in Fig. 4.1.

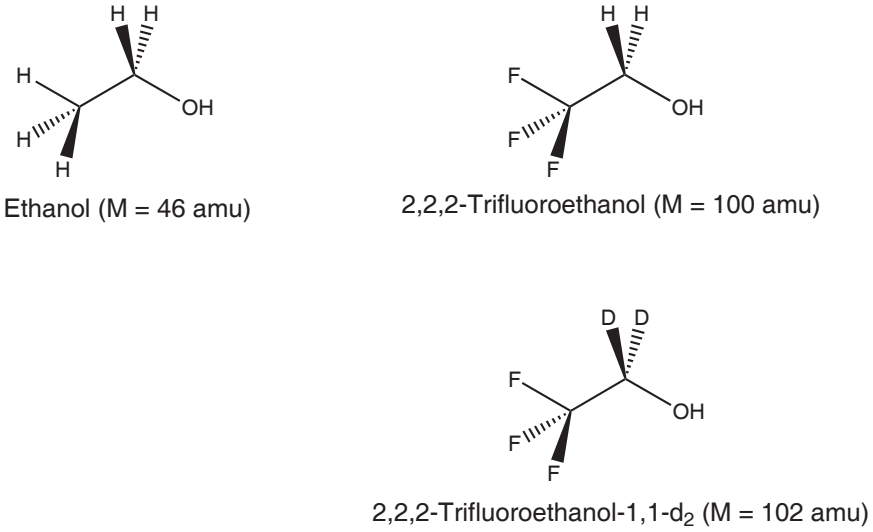

Figure 4.1: Molecular structure of the two investigated alcohols ethanol, 2,2,2-trifluoroethanol and its deuterated analogue.

Although the simplest alcohol methanol CH_3OH has been studied intensively in the last years [19, 48, 81, 96], there were to our knowledge no complete studies of DEA to ethanol or trifluoroethanol. For methanol it was shown that the decomposition into the three anionic products CH_3O^-, OH^- and O^- occurs via resonant processes at electron energies considerably above their thermodynamic thresholds [48]. The main resonance leading to the formation of these three fragments has a maximum at 10.2 eV. For the production of CH_3O^- two further resonances were detected at electron energies of 6.2 and 7.5 eV. All three resonances could be assigned as core excited Feshbach resonances (the formation of which goes along with electronic excitation) by the comparison of the He(I) photoelectron spectrum

of methanol with the DEA spectrum. In this resonance the 3s Rydberg-like orbital is doubly occupied [96]. Experiments with the (partly) deuterated molecules CD_3OD, CD_3OH, CH_3OD, CH_2DOD showed that the formation of OH^-/OD^- is strongly subjected to hydrogen scrambling. The corresponding ion yields demonstrate that no particular site selectivity with respect to the initial target molecule was observed. In contrary to that, the loss of hydrogen/deuterium leading to the anion CH_3O^- occurs exclusively at the OH/OD-site. Regarding the results for H^-/D^--formation from methanol it was shown that this reaction passes via the same resonances as the CH_3O^- formation, namely at 6.3, 7.9 and 10.2 eV [81]. Experiments with CH_3OD further demonstrated that within the three detected resonances the first two ones at lower energy are related to the loss of H^-/D^- from the O-site, whereas the third one is assigned to H^- production from the C-site [19].

4.1.1 Simple bond cleavage in ethanol

Our experiments with ethanol lead to the formation of the negative ions OH^- and $CH_3CH_2O^-$ via the same resonance with a maximum at 8.2 eV and some weak contributions to the $CH_3CH_2O^-$ yield around 2 and 5.5 eV (see Fig. 4.2) [67]. There is also an indication for the formation of O^-, but in this case it cannot be excluded that it may also be a product of DEA to background O_2 or to impurities. A most recent study of DEA to ethanol was performed by *M. Allan and coworkers* [40] who reported as well the formation of the dehydrogenated anion $(M\text{-}H)^-$ and, furthermore, the production of the fragments $(M\text{-}H_n)^-$ with n = 2–6 but neither OH^-- nor O^--formation. The positions of the resonances leading to the product $CH_3CH_2O^-$ differ from that we detected as they found them to be at 2.88, 6.35 and 9.15 eV. If one has a closer look at their ion yields there is a shoulder observable at an energy around 8 eV that is in accordance with the main resonance observed in our experiments. *Allan and coworkers* assigned this resonance around 8 eV as a Feshbach resonance with a hole in the $\bar{n}_O$ oxygen lone pair orbital. They further assigned the resonance at 6.35 eV as well as a Feshbach resonance with a hole in the n_O oxygen lone pair orbital. The resonance at 2.88 eV was attributed to a very short-lived σ^*_{OH} resonance. The latter two resonances

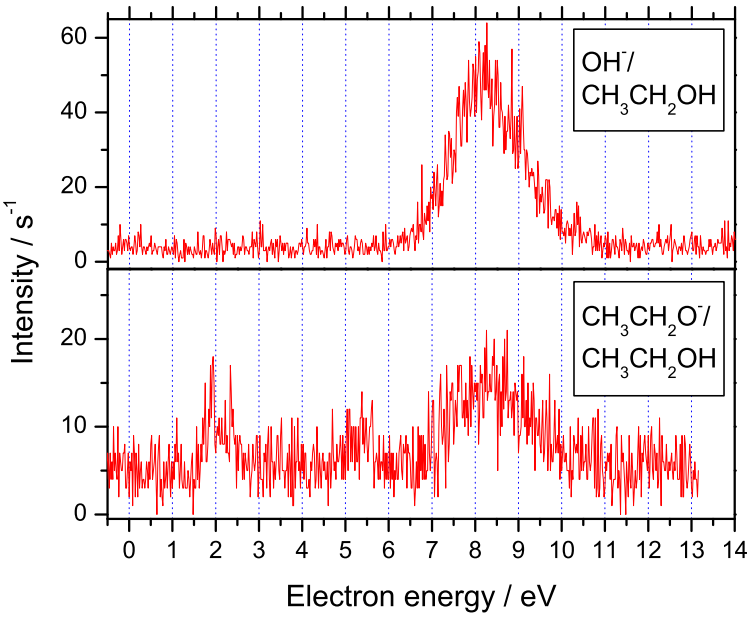

Figure 4.2: Ion yields for the fragments OH^- and $CH_3CH_2O^-$ arising from DEA to ethanol (p=$3{\cdot}10^{-5}$ mbar, $\Delta E \geqslant 300$ meV).

may be assigned to the features around 2 and 5.5 eV in our experiments although they are not exactly at the same energy. Due to the low intensity of the observed signal in our experiments, one cannot definitely conclude if there is a second resonance underlying the main peak for $(M\text{-}H)^-$ formation that would be in accordance with the resonance at 9.15 eV observed by *Allan and coworkers*. The remaining differences in the energy of the observed resonances are most likely due to the worse energy resolution of our electron beam that was $\geqslant$300 meV, whereas *Allan and coworkers* worked with 150 meV resolution. Nevertheless, there is a difference in the intensity ratio of the observed resonances that may be a result of working under different pressure conditions as well as different electron currents.

The formation of $CH_3CH_2O^-$ and OH^- can be expressed by the following reaction schemes:

$$CH_3CH_2OH + e^- \longrightarrow CH_3CH_2OH^{-\#} \longrightarrow CH_3CH_2O^- + H \qquad (4.1)$$

$$\longrightarrow OH^- + CH_3CH_2 \qquad (4.2)$$

The anion $CH_3CH_2O^-$ can only arise from a simple bond cleavage in the molecule. In accordance with the results for methanol most likely the O–H-bond is cleaved. Thus the thermodynamic threshold for the corresponding reaction is defined by the difference between the calculated O–H binding energy (4.42 eV [67]) and the calculated electron affinity of the alkoxide anion (1.87 eV [67]), which is in good agreement with an experimental value (1.68 eV [110]) derived from the appearance energy of ion pair formation in electron impact to $(C_2H_5)_2O$. The thermodynamic threshold becomes then 2.55 eV, which is above the lowest energy feature observed experimentally. The weak intensity of the signal at this energy may be explained by DEA to vibrationally excited target molecules.

For the formation of OH^- the C_2H_5–OH bond with a bond dissociation energy of 4.18 eV [67] has to be cleaved whereas the electron affinity of OH (1.82 eV [1]) is gained. Thus one arrives at a thermodynamic threshold of 2.4 eV for this reaction. This is considerably below the experimentally observed onset for the formation of OH^- that is around 6 eV. Therefore it is likely that the DEA process leads to the formation of more than one neutral fragment. A favorable decomposition pathway would be the additional production of ethene.

$$CH_3CH_2OH + e^- \longrightarrow CH_3CH_2OH^{-\#} \longrightarrow OH^- + C_2H_4 + H \qquad (4.3)$$

This process would require an energy of 3.82 eV (calculated with the heats of formation for ethene (52.5 kJ mol^{-1}), for the hydroxyl radical (39 kJ mol^{-1}) and for the hydrogen atom (218 kJ mol^{-1}) [1] which is still below the experimentally observed threshold so that the remaining excess energy has to be distributed between the formed fragments.

4.1.2 Abstraction of stable molecules from trifluoroethanol

While for ethanol mainly high energy resonances were observed, there is a quite intense low energy feature present in trifluoroethanol that leads to dehydrogenation of the molecule and the formation of the corresponding alkoxide anion $CF_3CH_2O^-$. The fragment OH^- that was observed with much higher intensity than $(M\text{-}H)^-$ for ethanol is now no longer detected. As new products the following fragments are observed mainly at higher energy: $[C_2F_2HO]^-$, $[C_2FO]^-$,

CF_3^- and F^-. The corresponding ion yields are presented in Fig. 4.3 and 4.4. One can easily identify several resonant features in the energy range between 1 and 11 eV. Generally, the nature of resonances can be divided into single particle resonances and core excited resonances. At low energy (≈0–3 eV) mainly single particle shape resonances are present, at higher energy (about electronic excitation of the neutral molecule) additionally core excited resonances are observable.

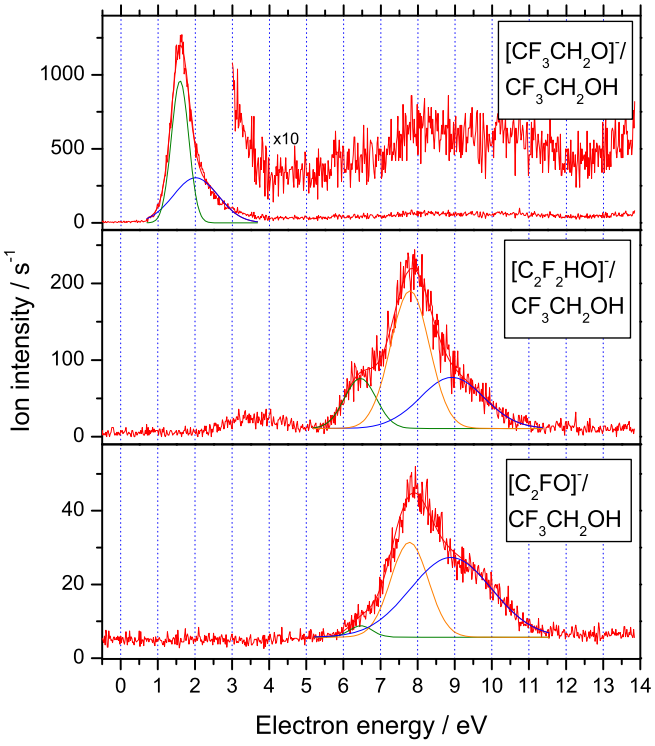

Figure 4.3: Ion yields for the fragments $[CF_3CH_2O]^-$, $[C_2F_2HO]^-$ and $[C_2FO]^-$ from DEA to gas phase trifluoroethanol, for $CF_3CH_2O^-$ magnification at higher electron energies by a factor of 10, fitted curves in green, orange and blue clarify the overlap of resonances (p=$2.7{\cdot}10^{-5}$ mbar, $\Delta E \geqslant 300$ meV).

A resonance with a maximum at 1.7 eV exclusively leads to the formation of $CF_3CH_2O^-$ by the loss of a neutral hydrogen atom.

$$CF_3CH_2OH + e^-(E \approx 1.7\,eV) \longrightarrow CF_3CH_2OH^{-\#} \longrightarrow CF_3CH_2O^- + H \quad (4.4)$$

Having a closer look on the ion yield for $CF_3CH_2O^-$, it is visible that the signal at low energy can be regarded as an overlap of two different resonances as clarified with help of the blue and green curves in Fig. 4.3. The estimated positions of these resonances are 1.5 and 2 eV and due to the arguments mentioned above they are assigned as shape resonances. Furthermore, the magnification of the ion yield at higher electron energy shows contributions in the energy range 5.5–14 eV with no clear structure. Experiments with the deuterated analogue CF_3CD_2OH show that hydrogen loss occurs exclusively from the O-site as only the $(M\text{-}H)^-$ anion was detected but not the $(M\text{-}D)^-$ anion. Thus this process shows a remarkable site selectivity.

Taking into account the calculated electron affinity for CF_3CH_2O of 2.74 eV and the calculated O–H binding energy of 4.47 eV, the thermodynamic threshold for the underlying reaction becomes 1.73 eV [67]. Due to the poor energy resolution used in these experiments because of weak ion intensities, this value is in good agreement with the experimentally observed energy with a peak maximum at 1.7 eV and an onset at ≈ 0.9 eV.

The other two fragments displayed in Fig. 4.3 are arising from multiple bond cleavage and the formation of new stable products. Formally the formation of the anion $[C_2F_2HO]^-$ goes along with the loss of two hydrogen atoms and one fluorine atom. For the production of $[C_2FO]^-$ the loss of three hydrogens and two fluorines is necessary. We assign these products to the loss of a hydrogen atom and the further abstraction of a new product hydrogenfluoride HF which is an extraordinarily stable molecule with a binding energy of almost 6 eV and therefore a favorable abstraction channel. Hydrogenfluoride abstraction frequently occurs in fluorinated compounds as will be shown for trifluoroacetic acid [53] and trifluoroacetone in the following chapters. We suggest the following two reaction pathways leading to product formation.

$$CF_3CH_2OH + e^- \longrightarrow CF_3CH_2OH^{-\#} \longrightarrow [F_2CCHO]^- + HF + H \quad (4.5)$$

$$\longrightarrow [FCCO]^- + 2\,HF + H \quad (4.6)$$

A possible structure for the anion formed by the abstraction of one HF and the loss of an H is the enolate $F_2C{=}CHO^-$. In case of the loss of two HF and one H the structure can be the acetyl ion $FC{\equiv}CO^-$. The thermodynamic threshold

for reaction (4.5) is given by E_{th} = D(C–F) + D(C–H) + D(O–H) - D(H–F) - EA(F_2CCHO) - E with E representing the energy of the rearrangement in the newly formed anion (e.g. for the formation of a double bond). By taking typical values for D(C–F)=5.0 eV and D(C–H)=4.4 eV, the calculated value from above for D(O–H)=4.47 eV and for D(H–F)=5.9 eV [108] the term E_{th} - EA(F_2CCHO) - E becomes 8 eV. The experimentally observed threshold is around 2.5 eV, and thus the difference of 5.5 eV is the minimum value that must be overcome by the unknown electron affinity of the corresponding radical and the rearrangement energy. An alternative way for product formation would be the abstraction of H_2 and F which would be energetically less favorable due to a lower binding energy of molecular hydrogen D(H–H)= 4.2 eV [1]. The formation of $[F_2CCHO]^-$ passes with comparable low intensity via a resonance around 3.5 eV and with higher intensity via a broad feature in the energy range between 5.5 and 11 eV. This broad structure is considered as an overlap of three different resonances with maxima at 6.4, 7.8 and 9.5 eV as shown by the fitted curves in Fig. 4.3.

The thermodynamic threshold for the formation of $[FCCO]^-$ is calculated in the same way as for the fragment $F_2C{=}CHO^-$, by taking into account the additional bond cleavage of a C–H and a C–F bond and the formation of a further HF molecule. Thus one arrives at E_{th} - EA(FCCO) - E = 7.1 eV which is only slightly above the experimentally observed appearance energy of the corresponding fragment. This small difference should be easy to overcome by the electron affinity and the rearrangement energy for e.g. the formation of a triple bond.

As additional fragments CF_3^- and F^- are observed, both arising from simple bond cleavage in the precursor molecule (see Fig. 4.4). The thermodynamic threshold for CF_3^- formation is calculated by taking into account D(C–CF_3)$\approx$4.3 eV [108] and EA(CF_3)$\approx$1.8 eV [21, 75] which results in $E_{th}\approx$2.5 eV. For F^- formation the threshold is calculated in the same way with the already mentioned dissociation energy for a C–F bond and EA(F)=3.4 eV [1] which results in $E_{th}\approx$1.6 eV. As especially CF_3^- is formed with surprisingly low intensity, it is difficult to determine the experimental appearance energy.

For F^- the thermodynamic threshold is in good agreement with experimental results. There are low electron energy contributions to the F^- yield although the more efficient fluoride formation occurs via resonant structures at higher en-

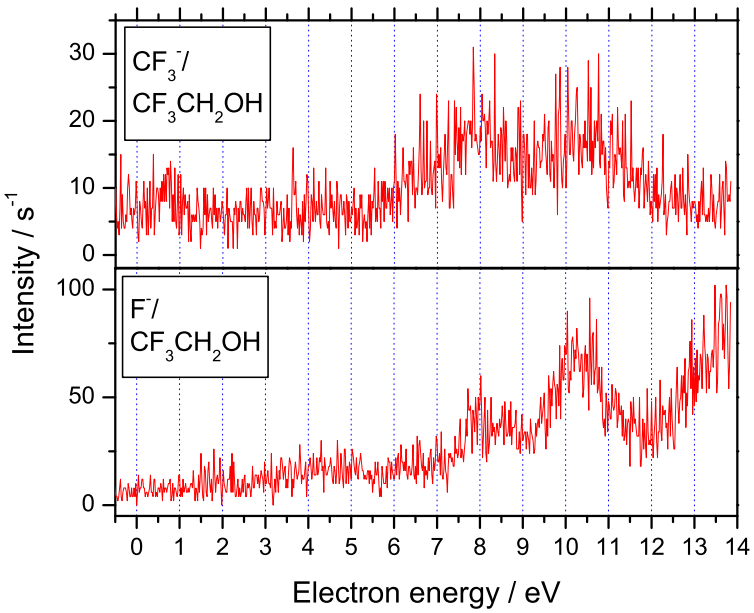

Figure 4.4: Ion yields for the fragments CF_3^-, F^- from DEA to gas phase trifluoroethanol (p=$2.7{\cdot}10^{-5}$ mbar, $\Delta E \geqslant 300$ meV).

ergies (≈8 and 10.5 eV). Above 12 eV the ion signal is continuously increasing, which is an indication for dipolar dissociation (ion pair formation) of the precursor molecule. This is a non-resonant process where the interaction with the electron creates a highly excited neutral molecule that decomposes into F^- and the corresponding cation $CF_2CH_2OH^+$.

4.1.3 Differences in electron attachment to fluorinated and non-fluorinated alcohols

The experiments with the partly fluorinated alcohol CF_3CH_2OH and ethanol CH_3CH_2OH clearly show that fluorination here increases considerably the cross-section for dissociative electron attachment. Furthermore, it can be summarized that ethanol forms exclusively products of simple bond cleavage while the fluorinated alcohol shows a tendency to abstract the stable molecule hydrogenfluoride.

Thus more complex chemical reactions are favored in trifluoroethanol in comparison with ethanol. As a common reaction channel of the two alcohols the loss of hydrogen and the formation of the considerably stable alkoxy anion can be mentioned.

4.2 Electron attachment to simple organic acids

Formic acid is the simplest organic acid with the molecular composition HCOOH. The simple structure has made this compound a favorable model system used in various experimental investigations and theoretical analysis. Furthermore, formic acid is present in the interstellar medium (ISM) [22, 43] and in the coma of comets like Hale-Bopp [88]. Therefore the study of electron interaction with this molecule is of high interest from an astrophysical point of view as it could play an important role in the synthesis of more complex organic molecules like amino acids or higher homologues of formic acid which are significant for astrobiology. Thus it is important to understand the basic processes of electron interaction with formic acid in the gas phase and also in molecular clusters where the influence of a molecular surrounding can be clarified. The intermolecular interactions are in this case comparably strong as the molecules are bound via hydrogen bonds. The formic acid dimer is a very stable double hydrogen bonded organic complex with an enthalpy of dimerization about -58.6 kJ·mol^{-1} (-0.6 eV) [16] and is therefore often considered as a prototype of such species [58, 63]. Besides the well-known cyclic structure of the formic acid dimer with an eight-membered ring there are experimental indications for a polar acyclic structure dominated by long-range dipole-dipole interaction that was observed in helium nanodroplets at a temperature of 0.37 K [59].

Previous experiments at the University of Innsbruck, Austria, on DEA to HCOOH in the gas phase showed the formation of three decomposition products which are the dehydrogenated formic acid anion $HCOO^-$, the oxygen anion O^- and the hydroxyl ion OH^- [79, 80]. The fragment formed with the highest intensity is $HCOO^-$ with a maximum in the ion yield at ≈1.25 eV and an estimated cross-section at the peak of the resonance of $1.7\pm0.6\cdot10^{-22}$ m^2. A peculiarity of the resonance profile for the signal $HCOO^-$ is the sharp onset and the structured high energy tail that were assigned to vibrational excitation of the formate ion. The O^- formation occurs at higher electron energy via a weak resonance around 7 eV and a second contribution with higher intensity at an energy above 8 eV. The production of the OH^- anion follows a resonant process around 7.5 eV. The cross-section for the formation of the two fragments O^- and OH^- is about

one order of magnitude lower than for $HCOO^-$. According to these estimated cross-sections formic acid can be considered as a weak electron scavenger.

4.2.1 Site selective hydrogen abstraction from single formic acid

From the results so far it is not clear which site is involved in the loss of hydrogen. This can occur at two different positions, at the C–H position or at the O–H position. Experiments with the two deuterated isotopomers of formic acid HCOOD and DCOOH (see Fig. 4.5) can clarify this point.

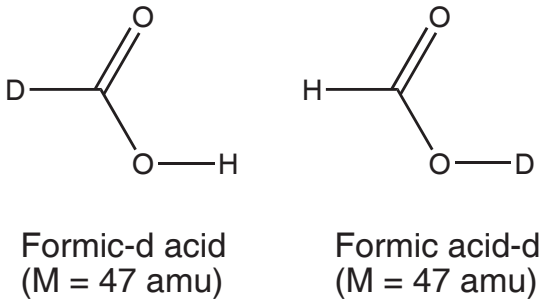

Figure 4.5: Molecular structure of formic-d acid and formic acid-d.

The experiments to study DEA to these isotopomers were performed at the *Comenius University Bratislava* in collaboration with *M. Stano* and *S. Matejcik* with an effusive beam electron attachment spectrometer [62] that is similar to the one described in Chapter 3.1.1. It consists of a trochoidal electron monochromator that interacts with an effusive beam, the negative ions arising from this interaction are detected by means of quadrupole mass spectrometry.

In Fig. 4.6 the ion yields for the carboxylate anions ($DCOO^-$ and $HCOO^-$) arising from electron interaction with the two isotopomers are shown. The corresponding reaction scheme is described for non-deuterated formic acid as follows.

$$HCOOH + e^- \longrightarrow HCOOH^{-\#} \longrightarrow HCOO^- + H \tag{4.7}$$

The carboxylate anion is formed via a low energy shape resonance with the additional electron occupying the lowest virtual state of π^* character localized

on the COOH group. This fragmentation can be observed at such low electron energy because of the considerable electron affinity of the HCOO radical (3.5 eV) [1]. Taking into account the binding energy of the O–H bond (4.87 eV) the thermodynamic threshold for this reaction becomes $\Delta H = 1.37 \pm 0.2$ eV [80].

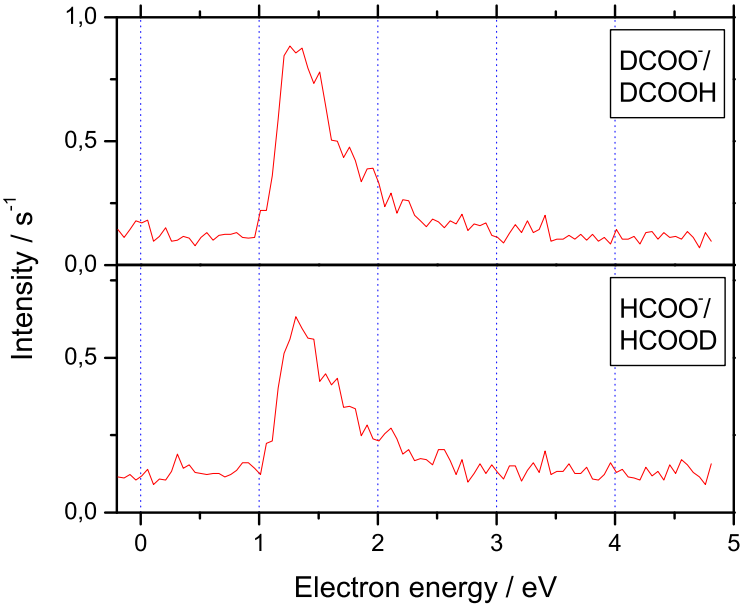

Figure 4.6: Ion yields for the two fragments $DCOO^-$ and $HCOO^-$ arising from DEA to DCOOH and HCOOD, respectively (ΔE=90 meV).

As can be seen from the mass spectra in Fig. 4.7 the formation of the carboxylate anion shows a remarkable site selectivity. For HCOOD almost exclusively a peak at 45 amu is detected whereas in case of DCOOH the major signal is at 46 amu. Thus one can conclude that the loss of H/D is almost exclusively observed from the O–H/O–D position. With an intensity of about 20 % of the main peak we also observe the formation of the anion $HCOO^-$/DCOOH and $DCOO^-$/HCOOD. These signals can either be due to an H/D exchange in the precursor ion and/or to some isotope impurities in the original sample. Such a site selectivity is not observed for HCOOH and some isotopomers in the condensed phase [94]. There the loss of H^-/D^- occurs via a broad resonance around 9 eV,

and the initial isotopomer looses its identity due to strong hydrogen/deuterium scrambling.

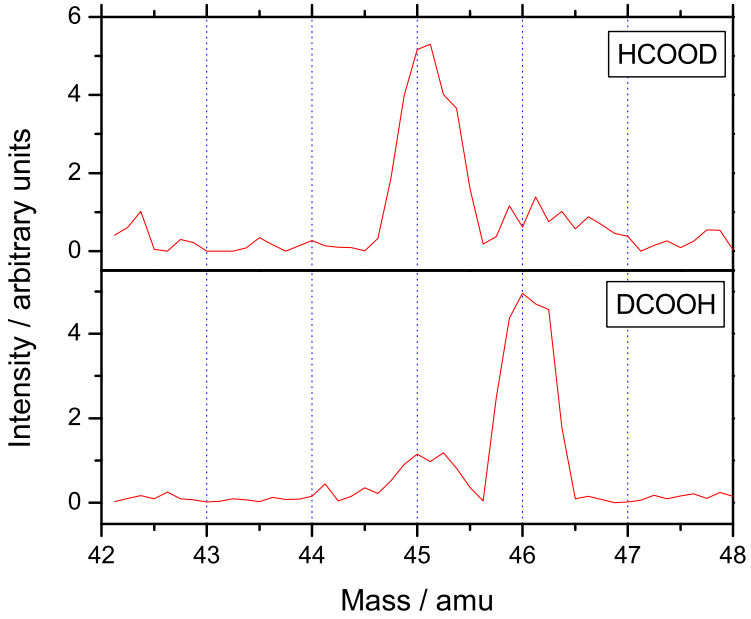

Figure 4.7: Mass spectra from HCOOD and DCOOH taken at an electron energy ≈1.3 eV (ΔE=90 meV) in the mass range 42–48 amu showing clearly a site selectivity of the dehydrogenation process.

Further experimental as well as theoretical studies on formic acid were recently performed by several other groups. *Prabhudesai et al.* detected H^- as a fourth fragment arising from electron attachment to isolated HCOOH in the gas phase with a maximum at an electron energy of 7.3 eV [82]. They assigned the corresponding resonance to be a core excited resonance as the first strong band in the absorption spectrum of formic acid that has been attributed to the $n_0' \rightarrow \pi_3^*$ excitation lies around 55000–61000 cm^{-1} (6.8–7.6 eV). Several publications reported on the nature of the resonances leading to decomposition of formic acid. Theoretical studies of *Gianturco and Lucchese* showed the presence of two distinct resonances that are ≈3 eV and ≈12 eV [27]. These values are higher than the experimentally observed resonances, but within the expectations for such scattering calculations

and thus in good qualitative agreement. They characterized the resonances as π^* intermediate with the excess electron entirely localized on the HCOO moiety. In the following the vibrational excitation energy is redistributed from the initially excited C=O and C–OH modes to the dissociative O–H stretching mode. Further studies on the dissociation mechanism were performed by *Rescigno et al.* and *Allan* [86, 6].

4.2.2 Formation of water in clusters of formic acid

Within the last years studies on DEA to DNA and RNA bases have shown that the dominant fragmentation channel is (like for gas phase formic acid) the loss of hydrogen via a low energy resonance around 1 eV [3, 4, 20, 29, 32]. More detailed investigations with deuterated thymine demonstrated that dehydrogenation occurs exclusively at the N-sites [2, 83, 84]. In the intermolecular hydrogen bond system that couples the bases in DNA one of these N–H bonds is involved. The question is whether a bond cleavage is still effective if the corresponding bond is participating in a comparably strong intermolecular hydrogen bonding. For this reason the investigation of the formic acid dimer as a simple model system is of high interest. These studies can thus provide information on the influence of a hydrogen bond on electron initiated reactions.

In Fig. 4.8 and 4.11 the negative ion mass spectra obtained from electron attachment to HCOOH and HCOOD are displayed. The first obvious and striking difference in comparison to the gas phase experiments is a dramatic increase in ion intensity. Considering the experimental arrangement in the cluster experiment where the collision zone is located in about 7 cm distance from the skimmer, and the fact that formic acid is mixed in a ratio of 1:100 in He, the particle density in the reaction zone is estimated to be lower than in the gas phase experiment. Thus one can conclude by comparing the count rates in the two measurements that the cross-section for electron attachment to clusters of formic acid is at least three orders of magnitude higher than for gas phase formic acid.

In the observed spectra the homologous groups in the monomer, dimer, trimer and tetramer region and some prominent peaks between these groups can be identified. Regarding the group around the monomer for HCOOH clearly the

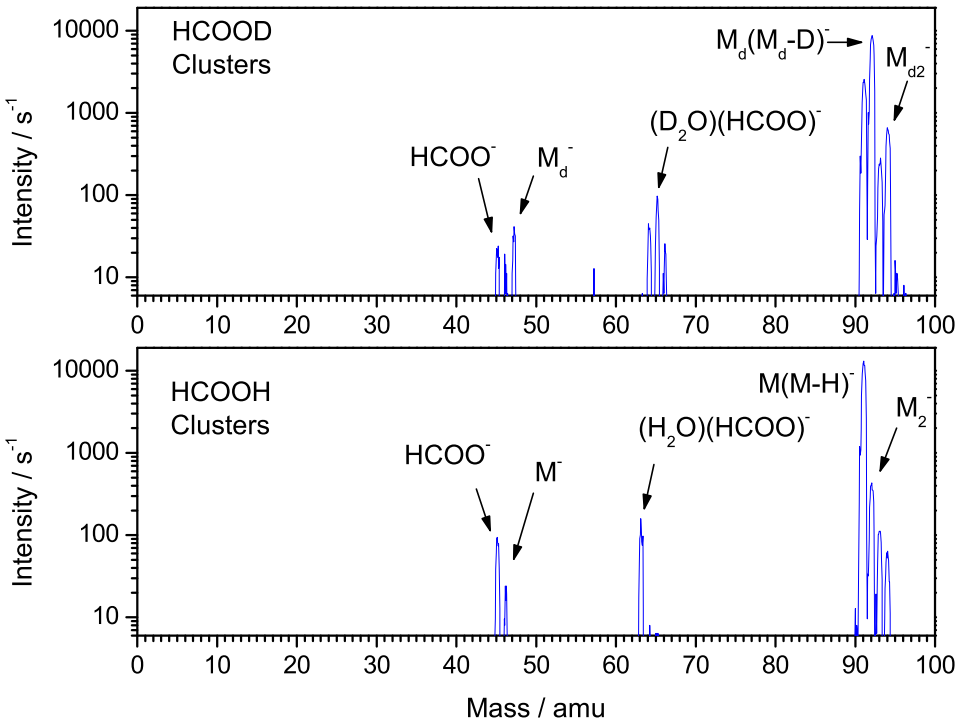

Figure 4.8: Negative ion mass spectra from HCOOD (upper panel) and HCOOH (lower panel) clusters taken at an electron energy of 1 eV in the mass range 0–100 amu (Mixture 1:100 in He, p=1 bar, ΔE=200 meV).

$HCOO^-$ ($[M\text{-}H]^-$) ion that was also detected in the gas phase experiments is present in the spectrum. Here one cannot definitely conclude on the origin of this peak, it can be formed in a molecular cluster but it can as well be a product of single molecules of HCOOH traveling in the beam. As a second ion at mass 46 amu but with lower intensity the negatively charged intact molecular anion $HCOOH^-$ (M^-) is detected. This is an indication that formic acid possesses a positive electron affinity or that it is at least stable on a mass spectrometric time scale. The phenomenon to detect intact molecular anions following electron attachment to clusters, whereas they are not present in the gas phase experiments, is frequently observed. As explanation one can consider that the electron is captured to a larger cluster and with subsequent collisional stabilization and evaporation of molecules the molecular anion is formed. The overall process is

hence named evaporative electron attachment. The observed dehydrogenation and the formation of M^- are confirmed by experiments with HCOOD, but there the intensity ratio between the two peaks is reversed, the intact molecular anion is now formed with higher intensity than the dehydrogenated acid. A small peak at 46 amu can either be attributed to $(M_d\text{-H})^-$ arising from some hydrogen exchange or to M^- due to isotope impurity of the sample.

In the region around the dimer similar signals are observed. There we find at mass 91 amu another product arising from dehydrogenation with the highest intensity within all detected anionic products that can be assigned to the $(M\text{-H})^-\cdot M$ complex. Again the intact molecular anion, in this case M_2^- ($M = 92$ amu) is formed by associative attachment. Additionally, two peaks at 93 and 94 amu are detected that are in the range of a few percent of the other peaks. The one at 93 amu may be assigned to the ^{13}C isotope, the other one to an ion-molecule complex originating from electron attachment to a higher order cluster (further details below). In agreement with the spectra of HCOOH the spectra of electron attachment to HCOOD show signals at 94 amu and at 92 amu that are attributed to $M_d\cdot(M\text{-D})^-$ and to M_{d2}^-. The peak at 92 amu could also contain some contributions of the structure $M\cdot(M_d\text{-H})^-$ or $M_d\cdot(M\text{-H})^-$ arising from hydrogen scrambling or isotope impurity in the sample. Along this line the peak at 93 amu may be due to the following compositions: $M_d\cdot(M_d\text{-H})^-$, $M_d\cdot(M\text{-D})^-$ or $M\cdot(M_d\text{-D})^-$. In contrary, there is only one possible assignment for the peak at 91 amu, namely $M\cdot(M\text{-H})^-$. This complex is detected with an intensity of about 30 % of the deuterated analogue and hence indicating isotope impurity.

Ion yield spectra corresponding to the formation of $(M\text{-H})^-\cdot M$ and M_2^- are displayed in Fig. 4.9. The reaction mechanism that leads to the formation of these products can be formulated as follows.

$$(HCOOH)_n + e^- \longrightarrow (HCOOH)_n^{-\#} \longrightarrow HCOO^- \cdot HCOOH_{n-1} + H \quad (4.8)$$

$$\longrightarrow HCOOH_m^- + k\ HCOOH \quad (4.9)$$

$$(n = m + k)$$

Dehydrogenation mainly follows electron attachment via the low energy resonance (maximum in the ion yield at 1.1 eV) that was already observed in the gas phase. But there are also some contributions at higher energy as shown by the

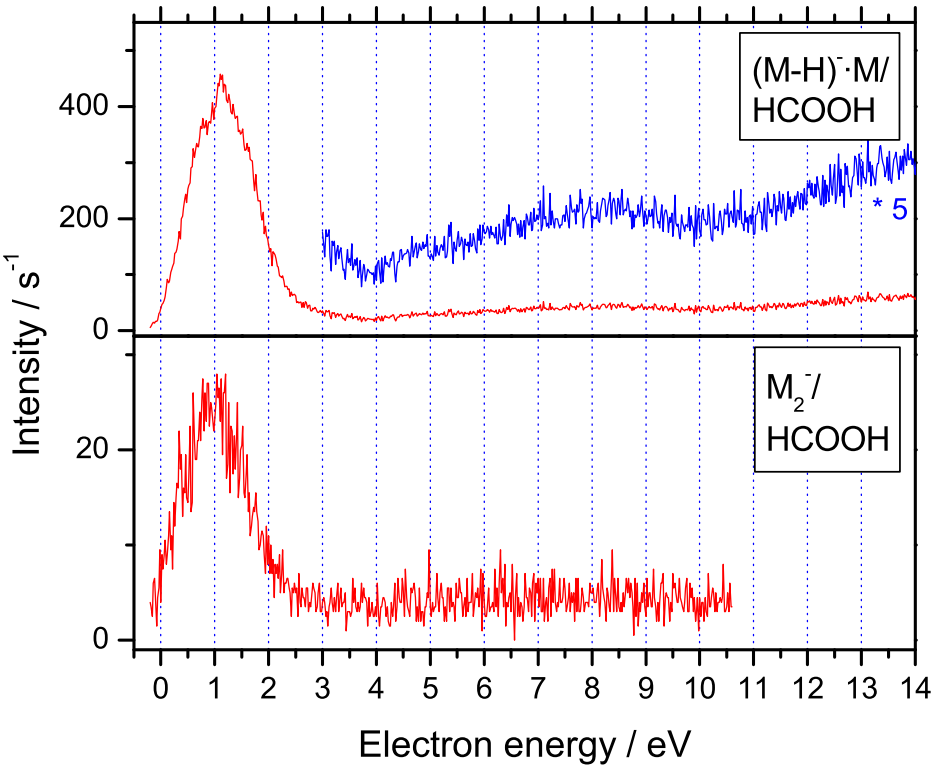

Figure 4.9: Ion yields for the formation of the anionic complexes $(M\text{-}H)^-\cdot M$ and M_2^- (Mixture 1:200 in He, p≈2.5 bar, ΔE=180 meV).

magnification in Fig. 4.9. In contrary the formation of M_2^- exclusively proceeds via the low energy resonance. This is in good agreement with calculations by *Gianturco et al.* [28] that predict three low-energy resonances in the region between 0 and 4 eV (two of them with π^* character). These calculated resonances possess realistic width and spatial features for the excess electron density distributions. They indicate the formation of the intact dimer anion as well as the loss of hydrogen as likely decay channels. Additionally, their results show a resonance around 9 eV as observed experimentally. Although the positions of the resonances do not differ appreciably in comparison to the monomer, *Gianturco et al.* propose that in this strongly bound dimer the electron density is no longer exclusively located

on an individual molecule in the cluster but on the entire dimer. Thus different resonances as for monomers may play a role.

Bachorz et al. [8] suggest an intermolecular proton transfer mechanism leading to the stabilization of the formic acid dimer anion. They propose that the excess electron is located in a π^* orbital which leads to a "'buckling"' of the molecular unit that accommodates the unpaired electron in order to suppress antibonding interactions. Due to the basic character of the anionic formic acid a proton is transferred from the second molecule of formic acid (acting as proton donor). This leads to the formation of the corresponding carboxylate anion and a dihydroxy radical as displayed in Fig. 4.10 and thus to the stabilization of the excess electron. The vertical detachment energy becomes then considerably high (2.35 eV). With respect to Gibbs free energy under standard conditions, the anion is more stable than the neutral by 37 meV. Experimental results that show a striking difference between the monomer and the dimer were recently published by *M. Allan* [6]. In this work it is demonstrated that the excitation of a vibrational quasicontinuum in the energy range ≈1–2 eV with the ejection of very slow electrons is about 20x more effective in the dimer. This may be explained with the help of the proton transfer mechanism mentioned above.

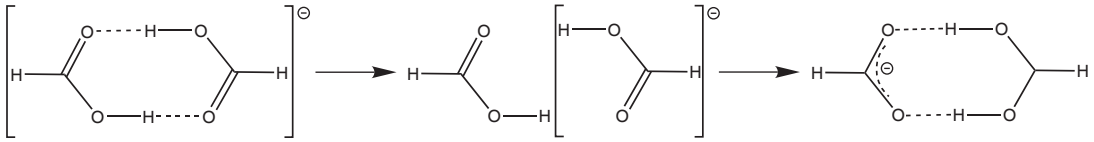

Figure 4.10: Proton transfer mechanism according to *M. Allan* [6].

The groups around the trimer and tetramer are assigned in the same way, there we observe as well the intact molecular anions M_3^-, M_4^- and the dehydrogenated complexes with the electronic structure $M_n \cdot (M\text{-}H)^-$ (n=3, 4) and the respective deuterated complexes. In the spectra for HCOOD the signal corresponding to the loss of deuterium shows the highest intensity in the dimer and trimer region, respectively. Despite the fact that also non-deuterated molecules and hydrogen loss can contribute to this signal, as explained above, one can conclude that H/D-loss preferable occurs at the O–H/O–D site as observed in the gas phase.

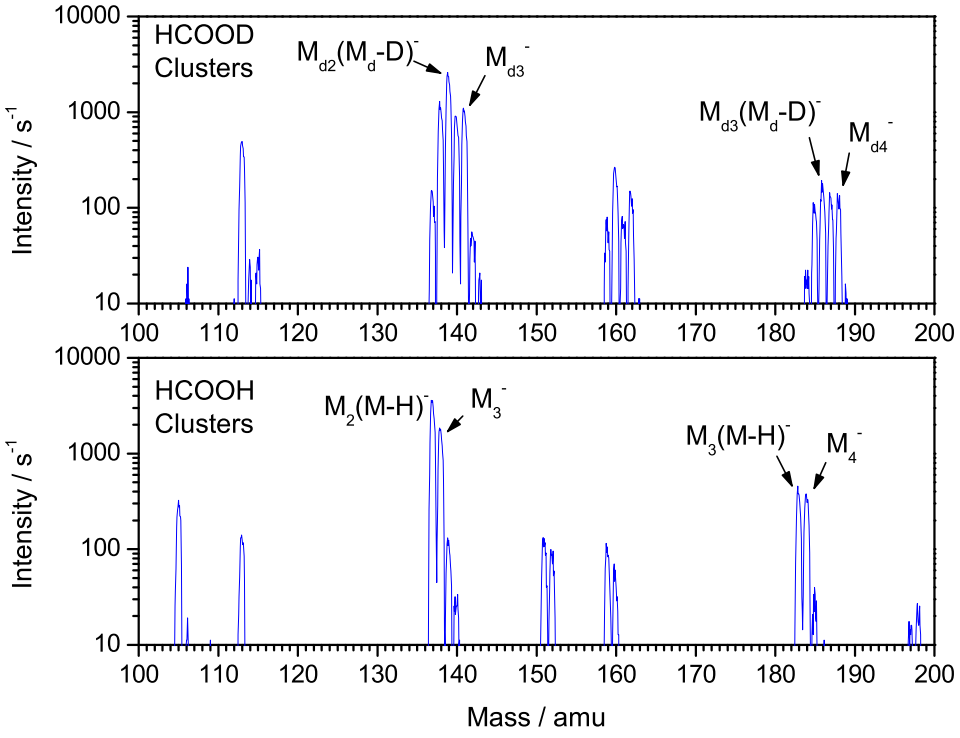

Figure 4.11: Negative ion mass spectra from HCOOD (upper panel) and HCOOH (lower panel) clusters taken at an electron energy of 1 eV (Mixture 1:100 in He, p=1 bar, ΔE=200 meV) in the mass range 100–200 amu.

A further interesting product with the mass 63 amu has a stoichiometric composition of $H_3CO_3^-$ which can be assigned to two likely electronic structures: $M{\cdot}OH^-$ or $H_2O{\cdot}(M\text{-}H)^-$. The thermodynamic threshold for the formation of OH^- calculated with the standard heats of formation of HCOOH, HCO and OH and the electron affinity of OH (ΔH_f(HCOOH) = 378.6 kJ·mol^{-1}, ΔH_f(HCO) = 43.5 kJ·mol^{-1}, ΔH_f(OH) = 38.99 kJ·mol^{-1}, EA(OH) = 1.8 eV) [1] is predicted to be 3.0 eV which is considerably above the experimental values. The production of the other possible product $H_2O{\cdot}(M\text{-}H)^-$ requires the formation of the carboxy-

late anion which was already shown for the gas phase to be possible at an energy ≈1 eV and further the cleavage of a C–O bond and the formation of the H–OH bond. Generally an H–OH bond (498 kJ·mol^{-1}) [108] is stronger than a C–OH bond (≈390 kJ·mol^{-1}) [60] which leads to the conclusion that only the second product can be formed at the respective electron energy. The overall reaction can then be formulated as follows:

$$(HCOOH)_2 + e^- \longrightarrow (HCOOH)_2^{-\#} \longrightarrow H_2O \cdot HCOO^- + HCO \qquad (4.10)$$

In this case the dissociated hydrogen does not leave the anionic complex as in case of dehydrogenation, but it forms with the OH group of the neighboring molecule a water molecule that remains attached to the carboxylate anion (see on the example of HCOOD in Fig. 4.12). This process can be considered as an intracluster intermolecular chemical reaction. Although the initial size of the cluster cannot be determined in this experiment, there are indications that this reaction exclusively follows electron attachment to the formic acid dimer as no higher homologues of the structure $M_n{\cdot}H_2O{\cdot}HCOO^-$ are observed. In the spectra of the deuterated isotopomer the peak corresponding to $D_2O{\cdot}HCOO^-$ is the one with the highest intensity in comparison to other isotope compositions. This is an indication that the formation of water preferentially occurs at the hydrogen bond site as shown in Fig. 4.12. *Ziemczonek and Wroblewski* propose two bound structures for this complex, a closed one where a six-membered ring is formed and an open structure where a new O–H-bond is formed between the carboxylate and the water [112].

A closer look at the mass spectra in Fig. 4.11 shows further signals in between the dimer and the trimer region and the trimer and the tetramer region. To simplify the analysis of these peaks only the non-deuterated compound is considered. The assignment of these peaks is not obvious, but they show a regular structure in that the peaks are 14 and 22 amu above the dimer and trimer region or 24 and 32 amu below the trimer and tetramer region respectively. To explain the origin of these signals one has to take into account that formic acid is thermodynamically a rather unstable compound as the decomposition into carbon dioxide and hydrogen is slightly exothermic by -14.5 kJ·mol^{-1}.

$$HCOOH \longrightarrow CO_2 + H_2 \qquad (4.11)$$

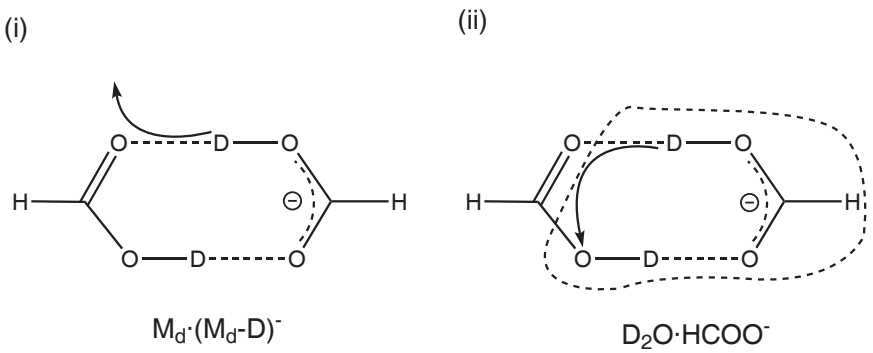

Figure 4.12: Schematic representation of the two reaction channels leading to (i) the loss of D thereby forming $M_d{\cdot}HCOO^-$ and (ii) the formation of water attached to the formate anion in the complex $D_2O{\cdot}HCOO^-$ following electron attachment to clusters of formic acid.

The reaction leading to the formation of water and carbon monoxide is slightly endothermic by $+26\,\mathrm{kJ{\cdot}mol^{-1}}$.

$$HCOOH \longrightarrow H_2O + CO \tag{4.12}$$

Whereas under neutral gas phase conditions these reactions may not play a role because of their high activation barrier, the presence of an excess electron can change the situation. The mentioned reaction products and also formaldehyde H_2CO (which is energetically at the same level as H_2 + CO) may then either be attached to the anionic complex or leave the complex. As an example the signals at 151 and 152 amu as well as at 159 and 160 amu are discussed (the corresponding peaks around 151 amu are not present in the spectrum of HCOOD). The signal at 151 and 152 amu may correspond to $(M_4\text{-}H)^-$ and M_4^- subjected to the evaporation of neutral compounds of 32 amu that can be CO + 2 H_2 or H_2CO + H_2. The peaks at 159 and 160 amu may be the result of a unit of 22 amu attached to the complexes M_3^- or $(M_3\text{-}H)^-$. In this case one can assume the possibility of attaching H_2O + 2 H_2. A similar assignment is possible for the already mentioned signals at 93 and 94 amu. Here an H_2 molecule remains attached to the intact or dehydrogenated anionic dimer, respectively. But as this discussion is rather speculative, it should not be extended too much. However, one can conclude from the experiments in clusters that electrons can induce interesting and quite complicated chemical reactions at extremely low energy.

The participation of the O–H-bond in the hydrogen bonds between the molecules does not suppress bond cleavage at this specific position, it rather facilitates the formation of new products following electron attachment.

4.2.3 Complex chemical reactions in clusters of trifluoroacetic acid

In addition to formic acid further simple organic acids like acetic acid [76, 78, 90, 11] and propanoic acid [76, 77] have been studied with respect to electron interaction within the last years in the gas phase as well as in the condensed phase. Due to their more complicated molecular structure these higher homologues of formic acid show a rich fragmentation pattern already in the gas phase. As demonstrated in the previous chapter on alcohols, fluorination of a molecule dramatically changes the electron induced chemical reactions. In case of the acids this was shown by *Langer et al.* in an article about low energy electron attachment to gas phase trifluoroacetic acid (for the molecular structure see Fig. 4.13) [53]. There they confirmed the tendency to abstract the very stable compound HF from molecules containing hydrogen and fluorine as observed for trifluoroethanol. In addition one could expect a similar reaction pattern as for formic acid, e.g. the formation of water. Thus the further investigation of this molecule in different states of aggregation is of high interest to find out more about electron induced chemical reactions at very low electron energy and the influence of fluorination of a carboxylic acid.

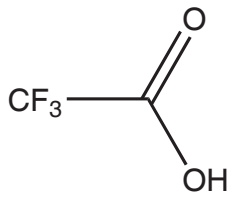

Trifluoroacetic acid
M = 114 amu

Figure 4.13: Molecular structure of trifluoroacetic acid.

As the results published by *Langer et al.* are the basis for the discussion of the results for molecular clusters and molecular films of CF_3COOH, they will be shortly summarized in the following. Dissociative electron attachment to trifluoroacetic acid leads to the formation of the anions CF_3COO^-, CF_2COO^-, CF_2^-, CF_3^-, F^- and probably some metastable CO_2^-. Among these fragments

CF_3COO^- and CF_2COO^- are observed with the highest intensity. They are formed via a low energy shape resonance near 1 eV that additionally leads to the formation of all the other fragments, but especially in case of CF_3^- and F^- with considerably lower intensity. A weaker resonance around 7 eV that yields F^- and CF_3^- was assigned as a core excited resonance. The corresponding ion yields taken from Ref. [53] are shown in Fig. 4.14.

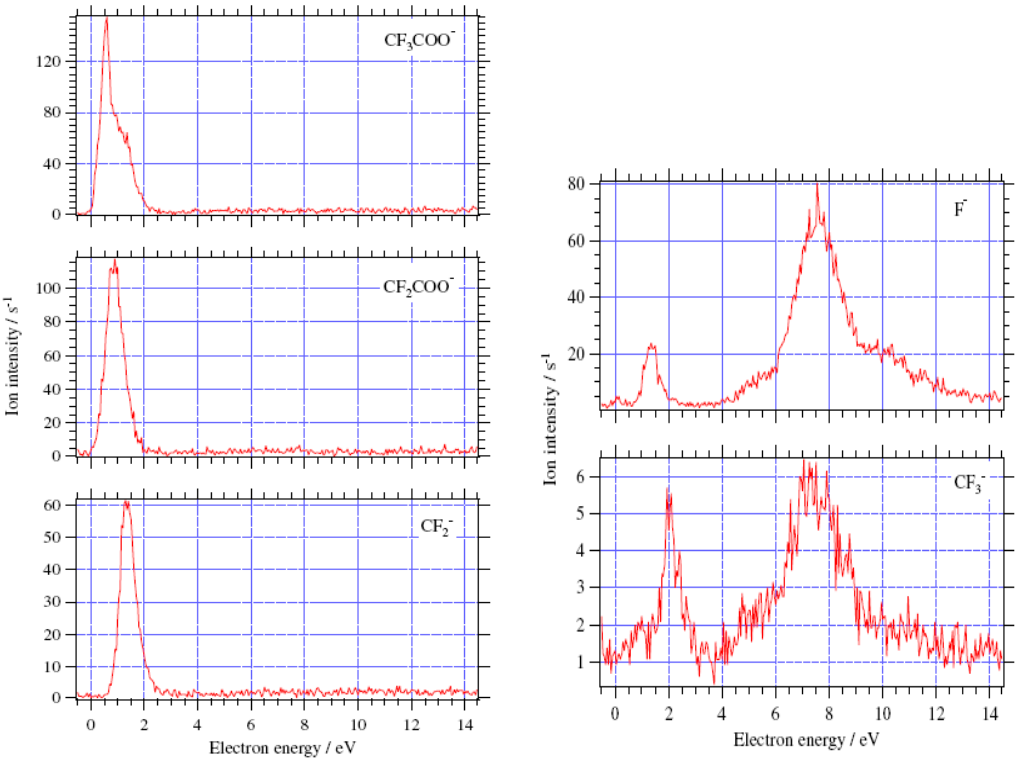

Figure 4.14: Ion yields for fragments arising from DEA to gas phase trifluoroacetic acid [53].

The fragments are formed via the following reaction mechanisms:

$$CF_3COOH + e^- \longrightarrow CF_3COOH^{-\#} \longrightarrow CF_3COO^- + H \quad (4.13)$$
$$\longrightarrow CF_2COO^- + HF \quad (4.14)$$
$$\longrightarrow CF_2^- + FCOOH \quad (4.15)$$
$$\longrightarrow CF_3^- + COOH \quad (4.16)$$
$$\longrightarrow F^- + CF_2COOH \quad (4.17)$$

These dissociation products of electron attachment partly arise from simple bond cleavage, but there are also more complicated reaction pathways that go along with multiple bond cleavage, rearrangement in the precursor ion and the formation of new molecules. As an example for such a complex chemical reaction the fragment CF_2COO^- is considered. In acetic acid the similar product CH_2COO^- was observed around 10 eV [78, 90] which is considerably higher than for the corresponding product from CF_3COOH. The formation of CF_2COO^- requires the cleavage of a C–F and the O–H bond, some rearrangement and the formation of the new molecule HF. The binding energy in HF is extraordinarily high and therefore the product can be observed already from the low energy shape resonance. Concerning the mechanism of product formation *Langer et al.* proposed hydrogen transfer in the precursor ion. *Zhong et al.* observed in ion cyclotron resonance (ICR) experiments with CF_3COOH also the ion CF_2COO^- and suggest that it is formed in a two-step mechanism [111]. First the ion-molecule complex $F^-{\cdot}CF_2COOH$ is formed, and in a second step the basic F^- abstracts the proton from CF_2COOH. In these experiments F^- is formed in the energy range 2.8–20 eV which is considerably above the energy observed for CF_2COO^- formation by *Langer et al.*, so that it is not likely in their case but cannot be completely excluded [53].

Electron attachment to trifluoroacetic acid clusters leads to the formation of a variety of anionic complexes. They are detected in groups around the monomer, the dimer, the trimer and the tetramer with a maximum in intensity in the region of the dimer. Thus this part is selected in the mass spectrum shown in Fig. 4.15. In accordance to the results of DEA to gas phase trifluoroacetic acid, dehydrogenation is as well operative in molecular clusters.

$$(CF_3COOH)_n + e^- \longrightarrow CF_3COO^- \cdot CF_3COOH_{n-1} + H \qquad (4.18)$$

The corresponding signals are located at 113 amu for CF_3COO^- and at 227 amu for $CF_3COO^-{\cdot}M$. Furthermore, the loss of hydrogen is observed for the trimer and tetramer (not shown here) but only at weak intensity. With higher order of the anionic complexes the formation of the intact molecular anions via associative electron attachment is more efficient than the loss of hydrogen.

$$(CF_3COOH)_n + e^- \longrightarrow (CF_3COOH)_m^- + k\ CF_3COOH \quad (n = m + k) \qquad (4.19)$$

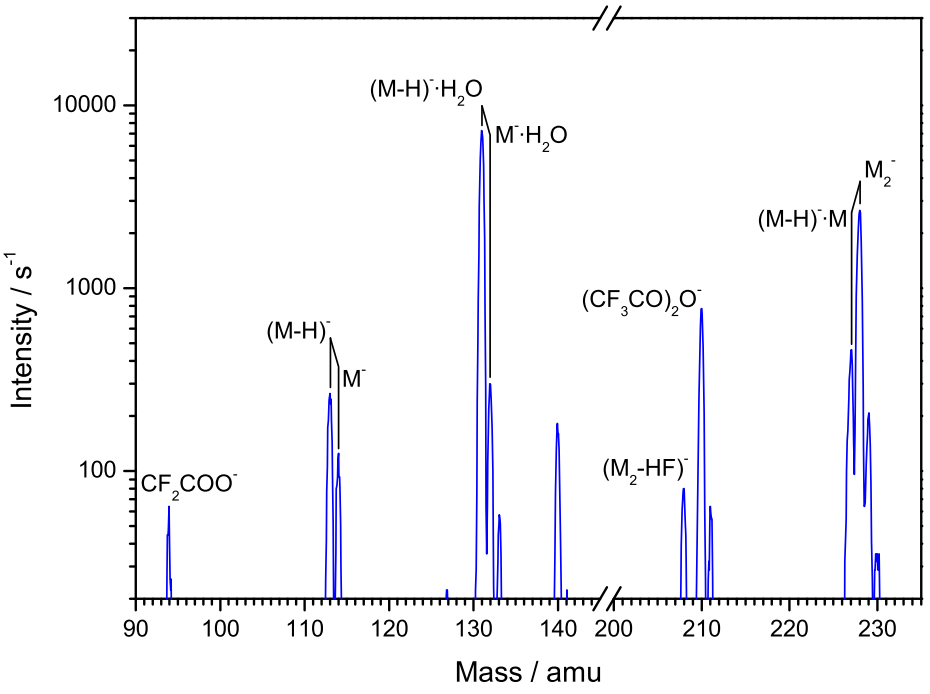

Figure 4.15: Negative ion mass spectrum of CF_3COOH clusters taken at an electron energy of ≈0.4 eV (Mixture 1:30 in Ar, p=0.5 bar) in the mass range 90–150 and 200–240 amu.

This mechanism is called evaporative electron attachment. Here electron attachment leads to the evaporation of k molecules from the initial cluster thereby stabilizing the anionic complex M_m^-. The detection of the intact molecular anion CF_3COOH^- is an indication that trifluoroacetic acid posseses a positive adiabatic electron affinity, while the vertical attachment energy is around 1 eV.

The signal at 131 amu corresponds to the formation of an anionic complex with the stoichiometric composition $C_2F_3H_2O_3^-$. One can propose two likely electronic structures for this complex: $OH^-{\cdot}CF_3COOH$ and $CF_3COO^-{\cdot}H_2O$. A similar result was observed for formic acid (see above), where the consideration of thermodynamical data revealed that only the second structure (formation of water) is possible at such low electron energy. As the energetic situation is quite

similar in case of trifluoroacetic acid, one can conclude that the formation of water is here as well an efficient process. Once the hydrogen is abstracted to form the carboxylate, only a C–OH bond needs to be cleaved ($\approx 390\,\mathrm{kJ{\cdot}mol^{-1}}$). The energy necessary for this bond rupture is more than compensated by the formation of the H–OH bond ($498\,\mathrm{kJ{\cdot}mol^{-1}}$) [1]. The corresponding complex $CF_3COO^-{\cdot}H_2O$ is formed with the highest intensity within all detected anionic complexes. This is different to the results for formic acid where dehydrogenation was more than one order of magnitude more efficient than the formation of water. Thus one can conclude that the introduction of the CF_3 group increases the tendency to undergo this chemical reaction. This is probably due to a weakening of the O–H-bond by the electron-withdrawing CF_3-group or to a larger binding energy of the complex $CF_3COO^-{\cdot}H_2O$ because of the large dipole moment of CF_3COOH (2.3 D) [108] and the high electron affinity of CF_3COO (4.2 eV) [56] that favors the chemical reaction from a thermodynamic point of view.

Similarly to formic acid, the formation of water is considered to be restricted to electron attachment to dimers because there are no contributions of complexes of the structure $CF_3COO^-{\cdot}M_n{\cdot}H_2O$ with $n \geqslant 1$ observable. Most likely effective energy dissipation in larger clusters, leading to the formation of M_n^-, suppresses the more complicated process of water production. However, one has to consider the signal at 132 amu which partly originates from the ^{13}C isotope. As its intensity is about 4 % of the peak at 131 amu it may also contain contributions of a complex $CF_3COOH^-{\cdot}H_2O$ which can only arise from electron attachment to a larger cluster. Nevertheless, water formation shows a remarkable size selectivity. As reaction mechanism one can imagine a similar process as for HCOOH that is initiated by the loss of hydrogen. But instead of leaving the complex to form $CF_3COO^-{\cdot}M_n$, the hydrogen runs into the OH-group of the neighboring CF_3COOH molecule thereby forming water. The polar water molecule remains then attached to the carboxylate anion whereas CF_3O is leaving the complex.

$$(CF_3COOH)_2 + e^- \longrightarrow (CF_3COO)^- \cdot H_2O + CF_3CO \tag{4.20}$$

An alternative route following the formation of water is the evaporation of the water molecule from the complex. The excccess charge is stabilized on the

rearranged remaining counterpart that is likely to represent the anhydride of trifluoroacetic acid (peak at 210 amu) $[(CF_3CO)–O–(COCF_3)]^-$.

$$(CF_3COOH)_2 + e^- \longrightarrow [(CF_3CO) - O - (COCF_3)]^- + H_2O \tag{4.21}$$

This product is also limited to water abstraction from the dimer, no higher homologues are observed, which is a further indication that only the specific configuration in the dimer allows the formation of water. An overview of the main reaction channels in trifluoroacetic acid clusters gives Fig. 4.16.

As further signals, the products of HF abstraction are observed. The anion CF_2COO^- (94 amu) observed in the gas phase is formed with considerable intensity. From these experiments it cannot be concluded whether the signal arises from electron attachment to a cluster or to single molecules traveling in the beam. Additionally, a signal at 208 amu is detected that can be assigned to $(M_2\text{-HF})^-$ which can only arise from electron attachment to a cluster. In this case HF may be abstracted from one molecule or it may be the product of an intermolecular reaction. The following reaction scheme can be proposed for this process. But due to the appreciable stability of CF_2COO^- [53] the formation of this anion solvated by a neutral molecule is more likely.

$$(CF_3COOH)_2 + e^- \longrightarrow (CF_2COO)^- \cdot M + HF \tag{4.22}$$

Again this reaction seems to be limited to HF abstraction from the dimer because no complexes of higher order are observable. But as the complex is produced in quite weak intensity, one cannot exclude that there may be as well higher order complexes which are below the detection limit.

In order to confirm that water formation is really a product of an intracluster chemical reaction and not due to some pick-up of water from the background in the expansion zone or impurities of the sample, experiments with the deuterated isotopomer of trifluoroacetic acid CF_3COOD were performed. A general problem arising in the work with deuterated compounds is that they can perform H/D-exchange in the gas inlet system and are thereby transformed into the hydrogenated analogue. To reduce this problem several series of fill and pump out cycles can be performed during which the walls get increasingly covered with the deuterated compound.

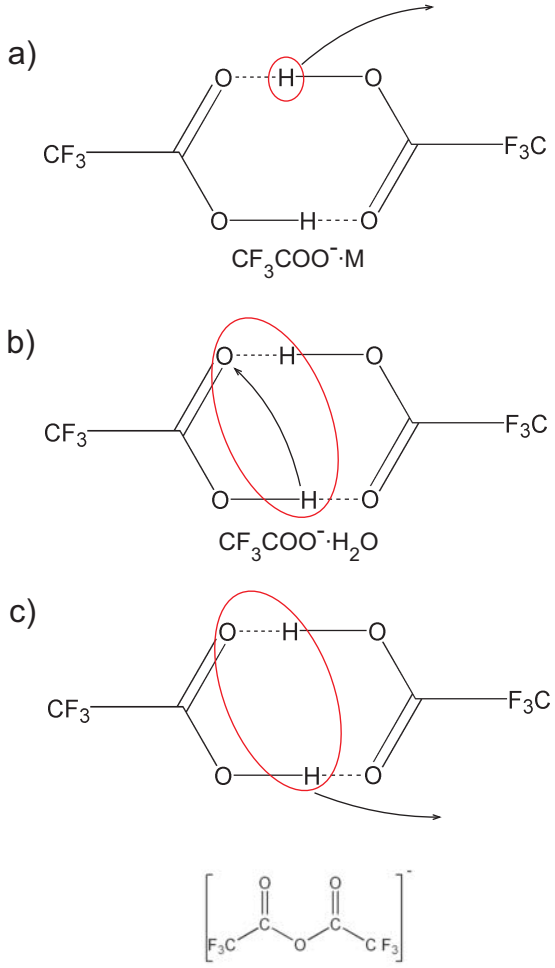

Figure 4.16: Cartoon showing the main reaction channels following electron attachment to a trifluoroacetic acid dimer: (a) hydrogen loss leading to $CF_3COO^-{\cdot}M$ (b) formation of water resulting in the complex $CF_3COO^-{\cdot}H_2O$ (c) loss of water thereby formation of the anionic anhydride $[(CF_3CO)–O–(COCF_3)]^-$.

In Fig. 4.17 two sections of the negative ion mass spectrum arising from the interaction of the electron beam with clusters of CF_3COOD are shown.

In the region around the water containing complex in the mass range 131–135 amu the peaks (enumerated from 1 to 5) can be assigned to the complexes consisting of the carboxylate anion or the parent anion solvated by a water molecule, respectively, in different isotope compositions. Peak 1 can be clearly associated with the complex $CF_3COO^-{\cdot}H_2O$. As the intensity of this peak is quite low in

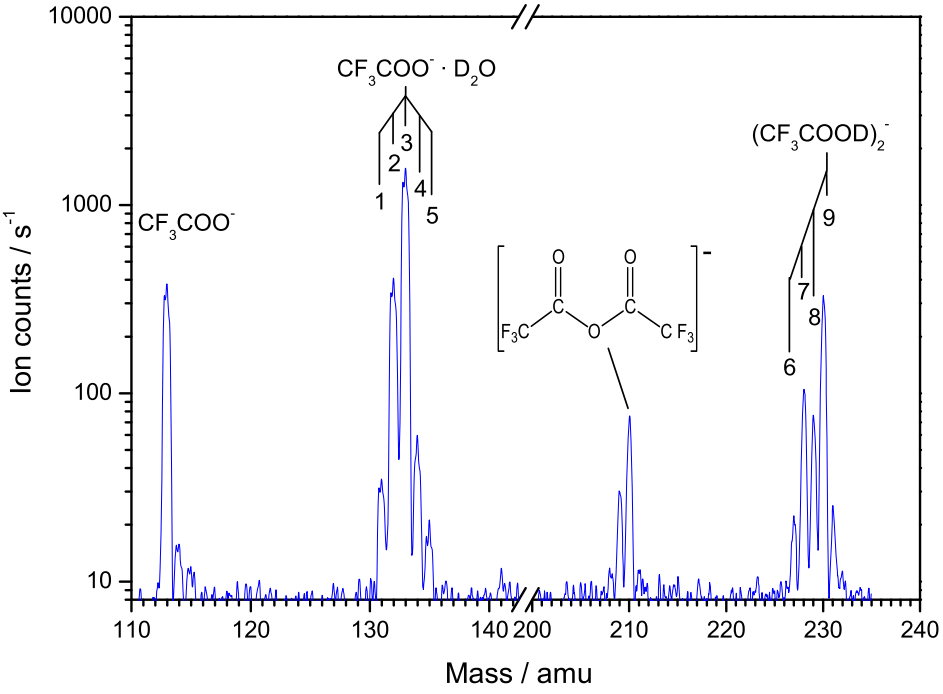

Figure 4.17: Negative ion mass spectrum of CF_3COOD clusters taken at an electron energy of ≈0.4 eV (Mixture 1:100 in He, p=1.5 bar) in the mass range 110–145 and 205–240 amu

comparison to the intensity obtained in the experiments with CF_3COOH one can conclude that the deuterated molecule was present in the beam in a considerable excess. The signal at 135 amu (5) can be assigned to $CF_3COOD{\cdot}D_2O$ and also some contributions of the ^{13}C isotope. The main peak at 133 amu is most likely due to the formation of the complex $CF_3COO^-{\cdot}D_2O$ but it can additionally include contributions of $CF_3COOD^-{\cdot}H_2O$ and $CF_3COOH^-{\cdot}HDO$. Thus we conclude that the formation of water definitely occurs in the molecular cluster as an intermolecular chemical reaction and is not due to some water pick-up from the background. The further peaks at 132 amu (2) and 134 amu (4) can be associated with the formation of $CF_3COO^-{\cdot}HDO$ or $CF_3COOH^-{\cdot}H_2O$ and $CF_3COOH^-{\cdot}D_2O$ or $CF_3COOD^-{\cdot}HDO$, respectively.

The second region from 227–230 amu displayed in Fig. 4.17 shows a series of peaks (enumerated from 6 to 9) arising from the dimer and its dehydrogenated form in different H/D-combinations. The dominant peak (9) at 230 amu can unambiguously be assigned to $(CF_3COOD)_2^-$ which is a further indication that the deuterated compound was present in the experiment in an excess. Further peaks that can be clearly identified are the peak at 227 amu with weak intensity (6) that can be assigned to $CF_3COO^- \cdot CF_3COOH$ as well as the one at 229 amu (8) which is due to $(CF_3COOH \cdot CF_3COOD)$. The peak at 228 amu (7) contains contributions of two different species and is a mixture of $CF_3COO^- \cdot CF_3COOD$ and $(CF_3COOH)_2^-$. A further weak signal is detected at 231 amu that is about 5 % of the one at 230 amu. Thus it is mainly attributed to the ^{13}C isotope.

Some selected ion yields are presented in Fig. 4.18. On the top panel the SF_6^- signal is shown which is used to calibrate the energy resolution. The other fragments are due to electron attachment to trifluoroacetic acid and can either arise from EA to clusters or to monomers traveling in the beam. A comparison with the gas phase results shows that the intensity ratio of the ions CF_3COO^-:CF_2^- changed to 50:1 in clusters while it is about 2:1 in the gas phase. Similarly the ratio for the formation of CF_2COO^-:CF_3COO^- changes from almost 1:1 for isolated trifluoroacetic acid to about 1:5 for clusters. The products CF_2^- and CF_2COO^- can only be formed by multiple bond cleavage and some rearrangement. Thus one can conclude that this more complex processes are suppressed in the cluster due to effective intermolecular energy transfer and that the abundance of monomers in the cluster must be very low (if present at all).

In clusters CF_3COO^- is additionally formed from the core-excited resonance around 7–8 eV which was not observed in the gas phase. With the present experiment it is not possible to distinguish whether this is a product of direct DEA from the core-excited resonance or a product of inelastic scattering in the cluster. In the second case the electron would be inelastically scattered by one molecule in the cluster and thereby slowed down. Then the slow electron would be captured by another molecule in the same cluster and dissociate into the observed fragment.

The ion yields presented in Fig. 4.19 show some anionic complexes that can only arise from EA to clusters of CF_3COOH. The formation of the complex

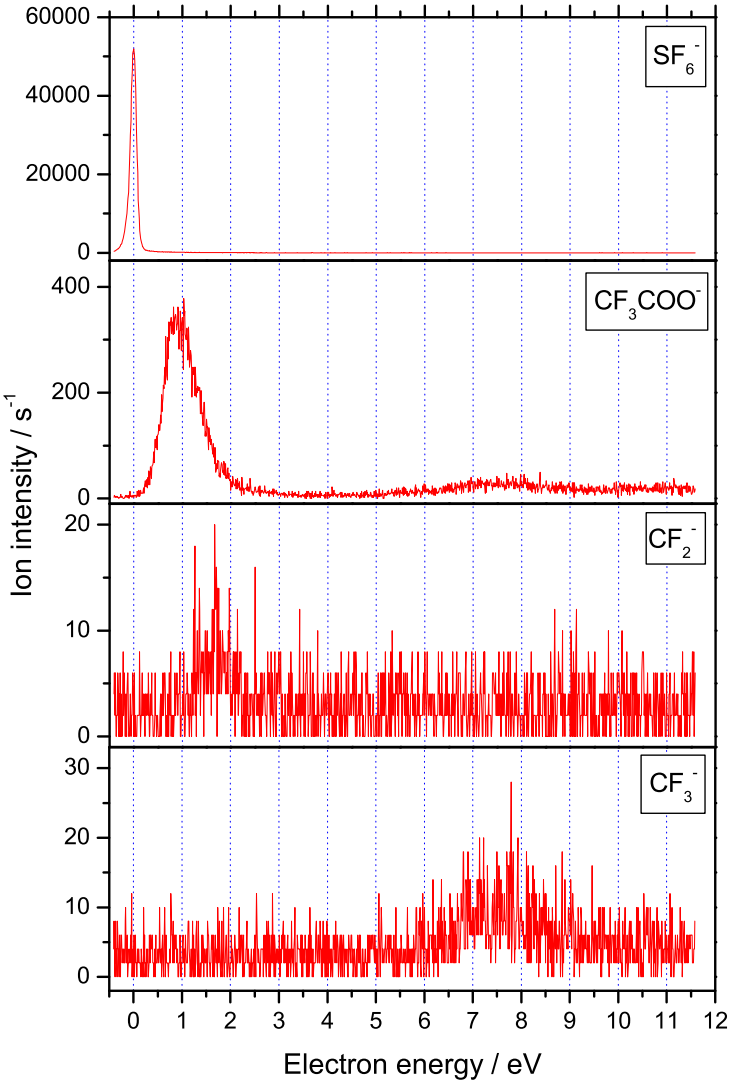

Figure 4.18: Ion yields for some selected fragments arising from electron attachment to CF_3COOD clusters (Mixture 1:30 in Ar p=0.5 bar, ΔE=160 meV)and for the calibration gas SF_6.

$CF_3COO^-{\cdot}H_2O$ has a maximum around 0.4 eV and is hence shifted to lower energy in comparison to the maximum of CF_3COO^- production. Generally, such a shift reflects the effect of solvation for an ion coupled to neighboring molecules. This means the initial Franck-Condon transition, leading to the formation of

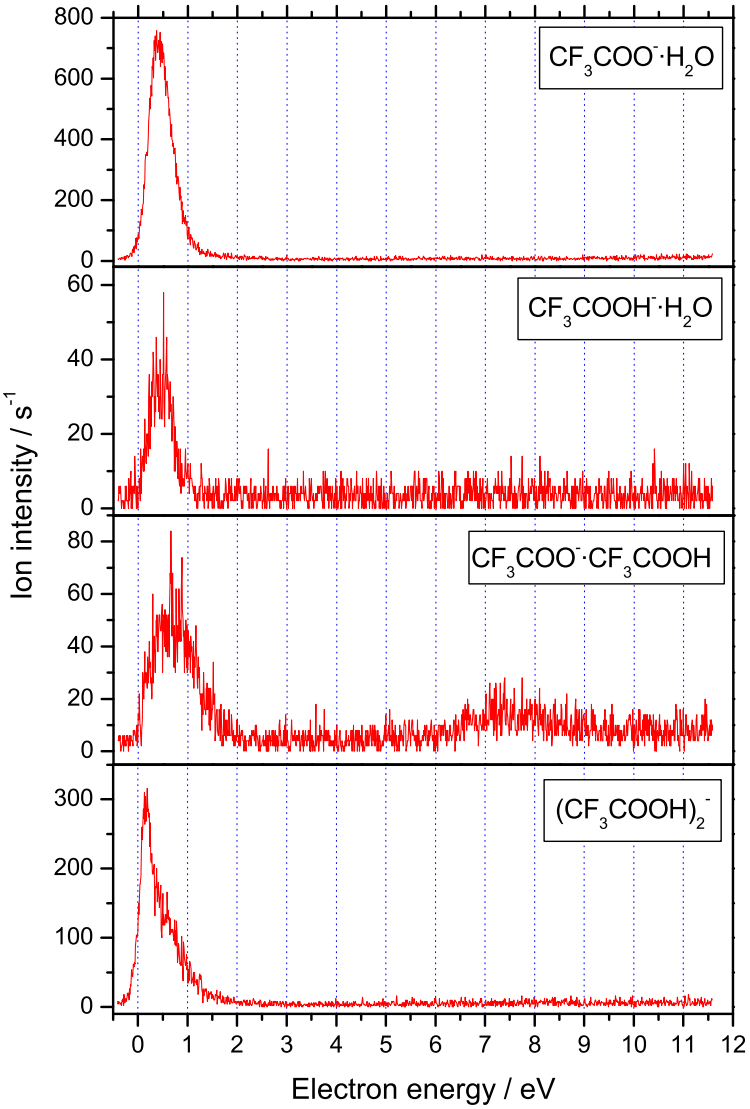

Figure 4.19: Ion yields for some selcted anionic complexes arising from electron attachment to CF_3COOD clusters (Mixture 1:30 in Ar p=0.5 bar, ΔE=160 meV).

the TNI, is subjected to a shift in energy which is then reflected in the ion yield of the corresponding product. The complex $CF_3COOH^-{\cdot}H_2O$ containing the intact molecular anion solvated by a water molecule is formed at the same electron energy as the corresponding dehydrogenated complex $CF_3COO^-{\cdot}H_2O$

with a maximum at 0.4 eV. Nevertheless, one has to take into account that for the complex with the trifluoroacetic acid anion a different mechanism has to lead to product formation. Here it cannot exclusively be a reaction within the hydrogen bonded dimer because of the additional hydrogen atom present in the complex. Therefore a third molecule needs to be involved.

Further products of electron attachment to trifluoroacetic acid are the dehydrogenated dimer $CF_3COO^-\cdot M$ and the dimer anion M_2^- as displayed in Fig. 4.19. The dimer anion is formed with considerably higher intensity than the dehydrogenated dimer anion. Whereas the maximum for the formation of $CF_3COO^-\cdot M$ is again at around 0.4 eV with further contributions in the range 7–8 eV, the maximum for the production of the intact dimer anion is shifted to 0.2 eV. This is again due to a solvation shift that indicates an appreciable stability of the dimer anion. Similar observations were made for the formation of CF_2COO^- and $CF_2COO^-\cdot CF_3COOH$. Here again the energy is shifted from about 1 eV for CF_2COO^- to 0.5 eV for the complex of $CF_2COO^-\cdot CF_3COOH$. Finally one should consider that in case of dimers additional resonances in comparison with the gas phase may be present. This was predicted by calculations of *Gianturco et al.* for the formic acid dimer. Here the excess electron density may not anymore be localized at an individual molecule in the cluster but distributed over the entire dimer.

4.2.4 Electron induced reactivity in molecular films of trifluoroacetic acid

Studies on electron stimulated desorption (ESD) of simple organic acids like HCOOH [94], CH_3COOH [11] and CF_3COOH [68] in the condensed phase show that the formation of H^- occurs for all three molecules via resonant features in the energy range above 5 eV. Trifluoroacetic acid additionally forms F^- in a similar energy region. These results show that electron interaction with this molecule indeed leads to fragmentation, but in ESD experiments only the negatively charged desorbing fragments are detected. Thus the question remains if there are also bigger negative ions formed by electron irradiation of the molecular films that cannot leave the surface due to the principle of momentum and energy

conservation. And furthermore, if these anions that remain on the substrate or the neutral counterparts (radicals) of some anionic fragments, can react further to some new products. As water formation was observed to be an efficient process in clusters of trifluoroacetic acid and formic acid, one would expect that similar reactions are possible in the condensed phase due to efficient intermolecular interactions. In fact there are indications for the formation of water observed by means of temperature programmed desorption (TPD) studies for condensed formic acid although only at considerably higher electron energy (7–8 eV) as in clusters (1 eV) [94, 50]. Additionally, for formic acid the production of CO_2 was reported above 8 eV while trifluoroacetic forms CO_2 and possibly CHF_3/CF_4 above 9 eV [68].

An interesting point is if these complex chemical reactions can also be induced via low energy resonances like in case of clusters. As trifluoroacetic acid is a more efficient electron scavenger than the non-fluorinated organic acids it is a promising approach to study whether analogous reactions can be identified in the condensed phase. To analyze the possible chemical reactions HREELS is used which offers the advantage to probe the film that remains on the surface after electron interaction without heating as in case of TPD. Thus the analysis of electron induced reactivity by means of HREELS allows to clearly distinguish between electron and thermal induced chemical reactions and therefore information complementary to TPD results is obtained.

The experiments to study CF_3COOH in the condensed phase were performed in close collaboration with the *LCAM (Laboratoire des collisions atomiques et moléculaire), CNRS - Université Paris-Sud, Orsay, France* [11]. The spectra in this chapter are generally recorded at temperatures around 30–40 K in specular geometry with an incident electron energy of $E_0 = 5$ eV and an energy resolution of $\Delta E = 5$–7 meV. Fig. 4.20 shows an HREEL spectrum of pure non-irradiated CF_3COOH. Each energy loss corresponds to the excitation of a characteristic vibration in the molecular film. The obtained values for the energy losses are in good agreement with those found in literature [9, 71, 85] and thus the assignment is done according to *Berney*.

The dominant peak in the spectrum is the loss at 150 meV that can be assigned to $\nu(CF_3)$. Besides the losses that can be clearly attributed to the excitation of

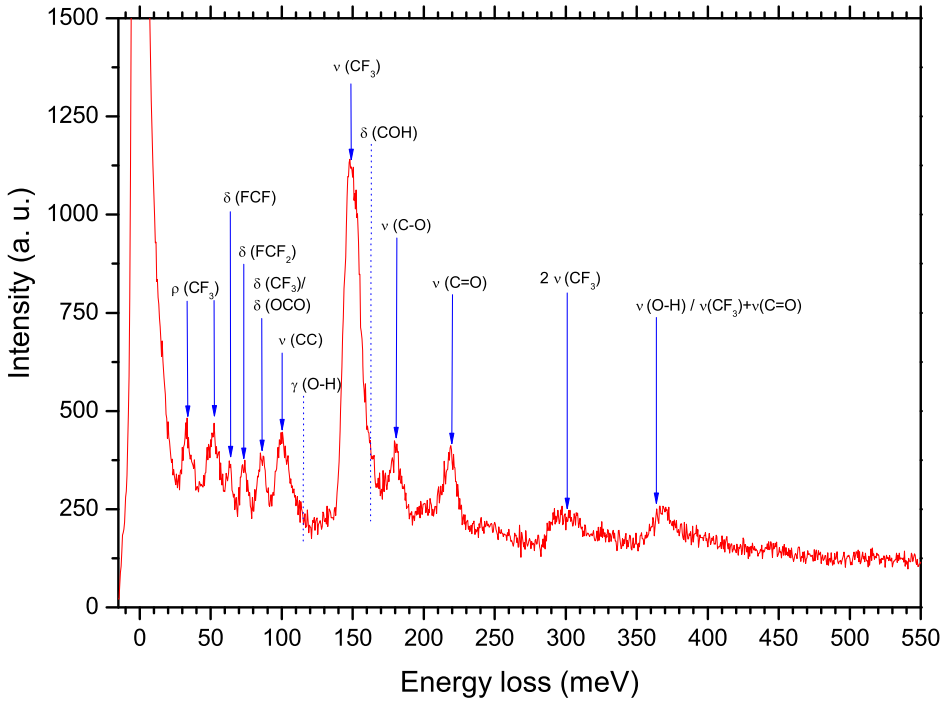

Figure 4.20: HREEL spectrum of a molecular film (4 ML) of pure non-irradiated trifluoroacetic acid, assignment of the characteristic losses according to *Berney* [9].

a specific vibration there are also overtones/combination modes observable. The loss at 300 meV is assigned to two times $\nu(CF_3)$ and that around 370 meV can either be attributed to ν(OH) or to $\nu(CF_3) + \nu$(C=O).

As the vibrational frequencies for the CF_3COOH monomer and the corresponding dimer substantially differ, one may generally distinguish if the OH-group is involved in such a hydrogen bonding network [85]. In case of CF_3COOH the corresponding losses cannot unambiguously be assigned to dimer organization because they are overlapping with other characteristic losses or combined modes. For example the ν(OH) related to dimer organization is at the same energy as the combined mode $\nu(CF_3) + \nu$(C=O). The situation is more clear in experiments with the deuterated isotopomer CF_3COOD. Therefore a comparison of

hydrogenated and deuterated trifluoroacetic acid is presented in Fig. 4.21. Here the ν(OD) and the δ(OD) for dimers are clearly observed whereas the τ(OD) is overlapping with ν(C–C). Hence the hydrogen bonding in the molecular films is clearly demonstrated. Also the effect of deuteration with respect to the energy of the corresponding losses is observable by the shift of the characteristic OH/OD modes to lower energy in case of deuterated trifluoroacetic acid.

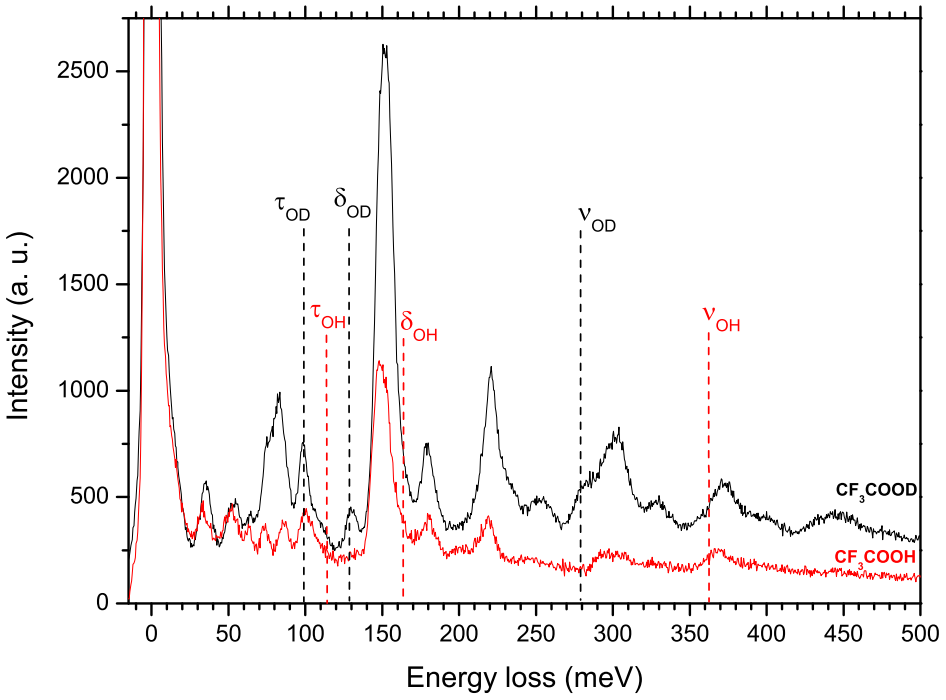

Figure 4.21: HREEL spectrum of a 4 ML molecular film of CF_3COOH and of a 8 ML film of CF_3COOD.

In Fig. 4.22 HREEL spectra of non-irradiated (d) and irradiated (c) CF_3COOH are displayed. The molecular films of CF_3COOH were irradiated with electrons of an energy of 1 eV and a dose of $1.3{\cdot}10^{16}\,e^-/mm^2$. The comparison of these two spectra shows that features present in the non-irradiated film disappear and new features appear after irradiation. These changes in the spectra and the interpretation of the underlying processes will be discussed in the following.

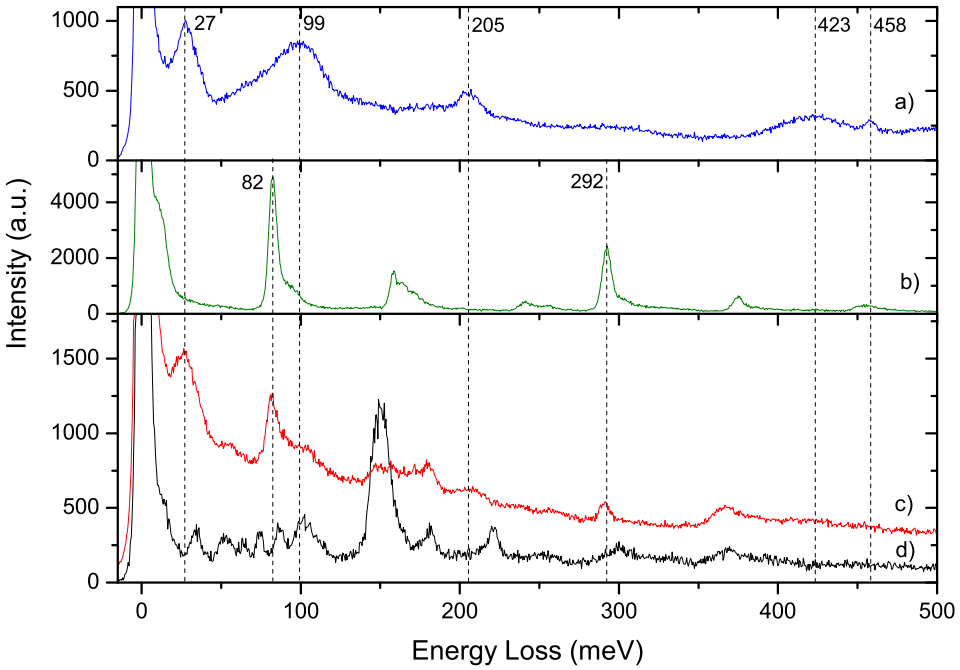

Figure 4.22: HREEL spectrum of molecular films (4 ML) of CF_3COOH non-irradiated (d), irradiated at an electron energy of 1 eV (c) and of the two compounds CO_2 (b) and H_2O (a).

On the first view one can easily identify the appearance of two new losses at 82 and 292 meV. The comparison with a spectrum of pure CO_2 shows that the newly observed peaks match with the two most intense losses in the spectrum of CO_2. Thus the new loss at 82 meV can be assigned to the deformation $\delta(CO_2)$ whereas the one at 292 meV is attributed to the asymmetric stretching $\nu_{as}(CO_2)$. In addition the loss at 220 meV (ν C=O) that is present in the spectrum of the non-irradiated acid is vanished after irradiation. Therefore one can conclude that the carboxylic group of the acid undergoes a chemical reaction to form CO_2 in considerable intensity at an electron energy of 1 eV.

Further new peaks are observable at 27 and at 205 meV and a broader feature around 100 meV. The comparison with the HREEL spectrum of H_2O clearly shows that these signals can be attributed to the translational phonon mode ν_T

(27 meV), the librational phonon mode ν_L (99 meV) and to the bending mode $\delta(H_2O)$ (205 meV). Thus one can conclude that in accordance to the results of CF_3COOH clusters the formation of water occurs in the condensed phase at comparable energy (≈ 1 eV).

Both of the two identified products can only arise from the carboxylic group. Thus there is still the question if the CF_3-group is also involved in a chemical reaction to form a new fluorinated product, or which are the co-products of water and carbondioxide formation. As the loss related to $\nu(CF_3)$ at 150 meV is a very intensive one it can provide important information on this point. The analysis of the observed spectra after irradiation reveals that this formerly dominant loss vanished almost completely after irradiation. Thus it is concluded that the CF_3-group undergoes further chemical reactions that lead to bond cleavage in this group. A likely co-product of CO_2 formation would generally be CF_3H which can be excluded in this case due to the absence of the characteristic loss for $\nu(CF_3)$. Further possibilities would be the formation of an AF-compound (some diatomic molecule which consists of some atom A and a fluorine F). A likely strucutre for the AF-compound would be HF that was considered to be a product of CF_2COO^- formation in the gas phase as well as in clusters. Although HF would show characteristic losses within the measured energy range, it may not stick on the surface at temperatures around 35 K. Furthermore, the formation of water already needs a considerable amount of the available hydrogen so that the production of HF may be operative to some degree but it cannot exclusively explain the dramatic change in the spectrum considering the CF_3-loss. Thus we propose the additional formation of some CF_x compound consisting for example of CF_2-groups. Due to an overlap of the characteristic losses for CF_2 with losses of CO_2 and/or H_2O it cannot definitely be identified.

To get further information on the mechanisms that lead to the formation of these products an energy dependent study was performed with a focus on CO_2 production. The HREEL spectra obtained after irradiation at five different energies (1, 2.5, 7, 11 and 20 eV) are displayed in Fig. 4.23, section I.). The two other sections are magnifications of the characteristic energy regions where new peaks corresponding to $\delta(CO_2)$ (II.) and $\nu_{as}(CO_2)$ (III.) should appear in case of CO_2-formation. These new losses are clearly observable after irradiation at

1 and at 20 eV indicating that CO_2 is efficiently formed in these cases whereas the spectra do not change significantly following irradiation at 2.5 and at 7 eV. After irradiation at 11 eV one can identify the presence of a loss corresponding to $\nu_{as}(CO_2)$ in weak intensity while it is not clear for the loss related to $\delta(CO_2)$. This is an indication that CO_2 formation occurs only in weak intensity. In a further irradiation experiment at 15 eV (not shown here) CO_2 formation is as well observed with considerable intensity.

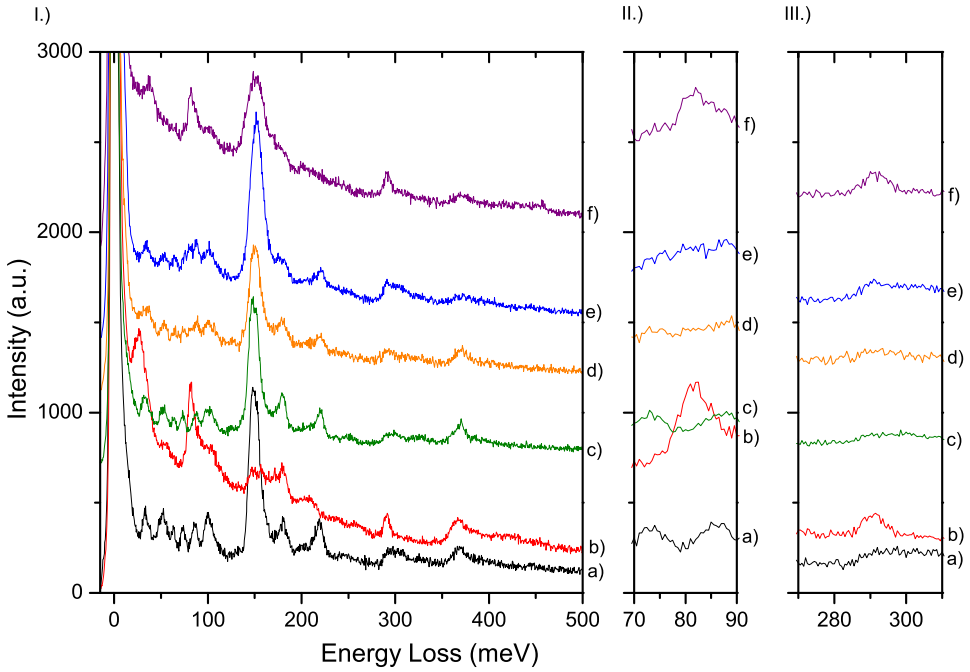

Figure 4.23: Section I. shows HREEL spectra of molecular films (4 ML) of CF_3COOH non-irradiated (a), irradiated at an electron energy of 1 eV (b), 2.5 eV (c), 7 eV(d), 11 eV(e) and 20 eV (f). In section II. the energy region around $\delta(CO_2)$ and in III. the range around $\nu_{as}(CO_2)$ are magnified.

These results allow some conclusions on the underlying mechanism of CO_2 formation. The efficient formation of CO_2 at 1 eV and the complete absence at 2.5 and 7 eV is an indication that it is formed in a quite narrow energy region around 1 eV, i.e. via a resonant process. At this energy DEA is the only accessible reaction channel. Furthermore, the presence of such a low energy resonance

around 1 eV is in accordance with the results from gas phase and molecular clusters as described in the previous chapter. Based on the article of *Langer et al.* around this energy the following anionic fragments are formed in the gas phase: CF_3COO^-, CF_2COO^-, CF_2^-, in weak intensity CF_3^- and F^- [53]. The authors also propose the formation of an anion of the structure CO_2^- or HCO_2^- that is mainly formed via a resonance at higher energy ($\approx$ 8 eV) but there might be as well contributions at low energy that cannot clearly be identified due to the weak intensity of this anion. The CO_2 formed in the condensed phase can hence be a product of multiple bond cleavage following electron attachment via a low energy resonance.

Secondly, CO_2 formation is observed at higher energies, namely at 15 and 20 eV and at 11 eV in weak intensity. In this energy range ionization and electronic excitation play a role and hence dissociative excitation or ion pair formation can lead to the production of CO_2. Since the results do not show a resonant behaviour at higher energy the mentioned non-resonant processes are most likely involved in CO_2 formation in this case. As CO_2 is observed at 11 eV only in weak intensity we propose that the threshold for non-resonant CO_2-formation is around this energy.

We thus finally conclude that CO_2 formation occurs via two different pathways, a resonant one at low energy and a non-resonant one at higher energy. The observation of non-resonant CO_2 formation at higher energy is in good agreement with the results of *Orzol et al.* [68] where the threshold for CO_2 formation is proposed to be around 9 eV.

Considering the mechanism for the formation of water the series of spectra in Fig. 4.23 clearly show that there is an energy region (2.5 and 7 eV) where no major changes are observed after irradiation of the molecular films. Thus also the formation of water as demonstrated in Fig. 4.22 is considered as a resonant process that goes along with the formation of a temporary negative ion at an electron energy of $\approx$1 eV. This result is in good agreement with the results obtained for molecular clusters where water formation around 1 eV was a very efficient chemical reaction.

Taking the 20 eV irradiation as an example for the non-resonant product formation it is an interesting point if the formation of water occurs as well at high

energy or if it is a specific reaction within the resonant feature around 1 eV. Fig. 4.24 shows a comparison between the non-irradiated film of CF_3COOH (c), the spectrum after irradiation at 20 eV (b) and a spectrum of pure H_2O (a). This comparison shows that the loss around 99 meV after irradiation may be attributed to the librational phonon mode ν_L of water. The loss at 205 meV ($\delta(H_2O)$) is not clearly observable and the loss at 27 meV (ν_T) is not present. The weaker losses at higher energy that are related to the stretching vibrations of water are also not clearly visible, but this was neither the case for the 1 eV irradiation. We therefore suggest that formation of water may occur in weak intensity.

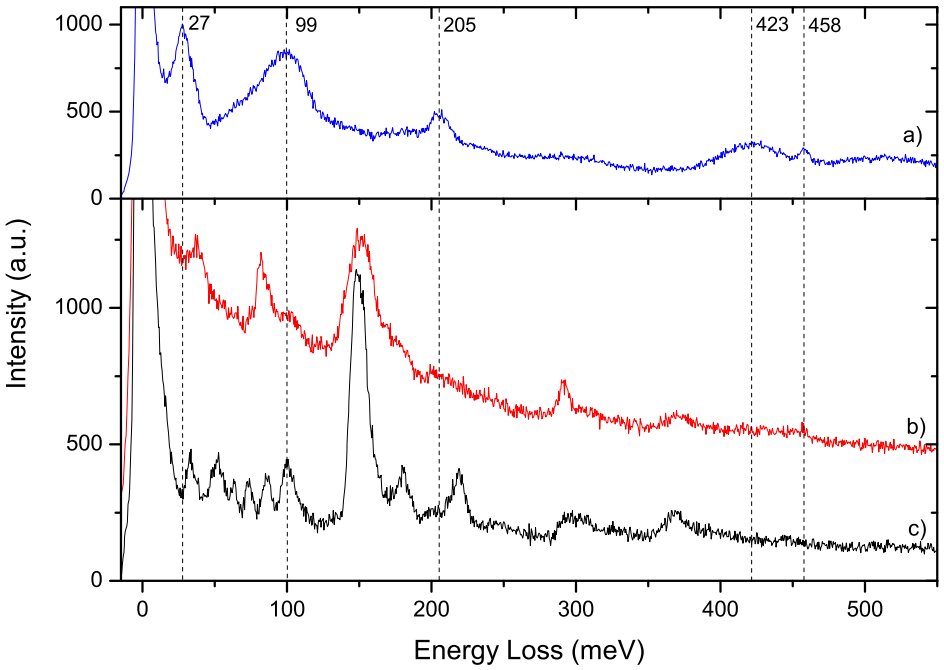

Figure 4.24: HREEL spectra of molecular films (4 ML) of CF_3COOH non-irradiated (c), irradiated at an electron energy of 20 eV (b) and a spectrum of pure water H_2O (a).

A look at the fluorinated group shows a different behavior when the molecular films are irradiated at 20 eV as opposed to 1 eV. After 20 eV irradiation the loss assigned to $\nu(CF_3)$ is still present so that the synthesis of some CF_3A compound

may occur during high energy irradiation. This observation is again in good agreement with the results of *Orzol et al.* as they propose the formation of CF_3H or CF_4 above 9 eV.

The following reaction scheme summarizes the two different reaction pathways leading to the various products.

$$\begin{aligned} CF_3COOH_{(s)} \; + \; e^-(E \approx 1\,eV) &\longrightarrow CF_3COOH^{-\#} \longrightarrow \\ CO_2 \; + \; H_2O + AF + CF_x + ... & \qquad (4.23) \\ CF_3COOH_{(s)} \; + \; e^-(E \approx 20\,eV) &\longrightarrow CO_2 + CF_3A + H_2O? + ... \qquad (4.24) \end{aligned}$$

The reaction mechanism (4.23) shows that the formation of a temporary negative ion via a resonant process at low electron energy leads to the formation of CO_2, H_2O, an AF- and a CF_x-compound. At higher energy a non-resonant process leads to product formation. CO_2 is formed via both reaction pathways in considerable intensity while the formation of water is much more efficient via the low energy resonant mechanism. Concerning the fluorinated group completely different products are obtained. The process at higher energy clearly leads to the formation of a fluorinated compound that consists of a CF_3-group which is not present after 1 eV irradiation. Here the production of an AF-compound and a CF_x-molecule is favored.

4.2.5 Common reaction tendencies for simple organic acids

The loss of hydrogen is a common reaction channel for formic acid and trifluoroacetic acid. In both cases this reaction is driven by the specific properties of the molecules that can form very stable carboxylate anions due to the high electron affinity of the corresponding radicals. The fluorination of a carboxylic acid leads like for fluorinated alcohols to the abstraction of the stable molecule HF.

The comparison of the results for clusters of the two organic acids shows that both molecules form water in an intracluster chemical reaction which is detected as a complex of the carboxylate anion solvated by one molecule of water. This process of water formation is the most efficient reaction pathway for trifluoroacetic acid while in formic acid the loss of hydrogen is still favored. Most likely the

specific configuration in a hydrogen bonded stable dimer allows the formation of water in both cases.

Experiments with trifluoroacetic acid in the condensed phase further show that the formation of water is also operative via a low energy resonance in this case. This is most likely again due to comparably strong intermolecular interactions by hydrogen bonds. Electron attachment via this low energy resonance additionally leads to the formation of carbondioxide and some fluorinated products that may be assigned to HF and some CF_x-compound. The formation of HF via the low energy resonance would be in good agreement with the results from gas phase and molecular clusters.

4.3 Carboxylic acid esters - the influence of esterification

The loss of hydrogen following low energy electron interaction is an ubiquitous process in many organic molecules including the DNA bases, amino acids and as shown in the previous chapters in alcohols and simple organic acids. In case of organic acids the driving force for this process can be seen in the very high electron affinity of the dehydrogenated acid radical, e.g EA (CF_3COO)= 4.2 eV [56]. Considering the DNA bases there is a similar situation. The ejection of a neutral hydrogen is here as well a favorable reaction due to a considerably high electron affinity of the dehydrogenated DNA bases in the range of 3–4.5 eV [83]. Calculations with the G2MP2 method of electron affinities of dehydrogenated thymine resulted in values slightly below 3 eV in case of loss from a C-position, for dehydrogenation at the N-position the values are even higher, namely 3.5 eV for ejection of hydrogen from the N1 position and 4.5 eV if the dehydrogenation occurs at the N3 position [20]. Experiments with deuterated thymine showed that hydrogen loss exclusively occurs at the N-sites [2]. Additionally, it was demonstrated that replacing H by CH_3 at the N1 position completely blocked the bond rupture at this specific position and the formerly observed stable anion is no more detected at the corresponding energy [84]. Although the bond breaking regarded in the case of thymine is dealing with a comparison of an N–H and an N–C bond, the question arises if a similar result can be obtained in case of trifluoroacetic acid by esterification of the acid (i.e. change of an O–H to an O–C bond). Thus it can be investigated if the formation of the stable acid anion is also blocked by the substitution of hydrogen with a hydrocarbon chain. The introduction of an ester group to avoid undesired chemical reactions is also a frequently used technique in organic chemistry (in liquids) [14, 106].

Furthermore, the analysis of the influence of the electronic nature of the introduced ester group on electron induced reactivity is of high interest. Therefore the investigation of three different esters of trifluoroacetic acid (CF_3COOCH_3, $CF_3COOC_2H_5$, $CF_3COOCH_2CF_3$) and of one complementary fluorinated ester of acetic acid ($CH_3COOCH_2CF_3$), see Fig. 4.25, was performed on single molecules in the gas phase as well as for molecular clusters.

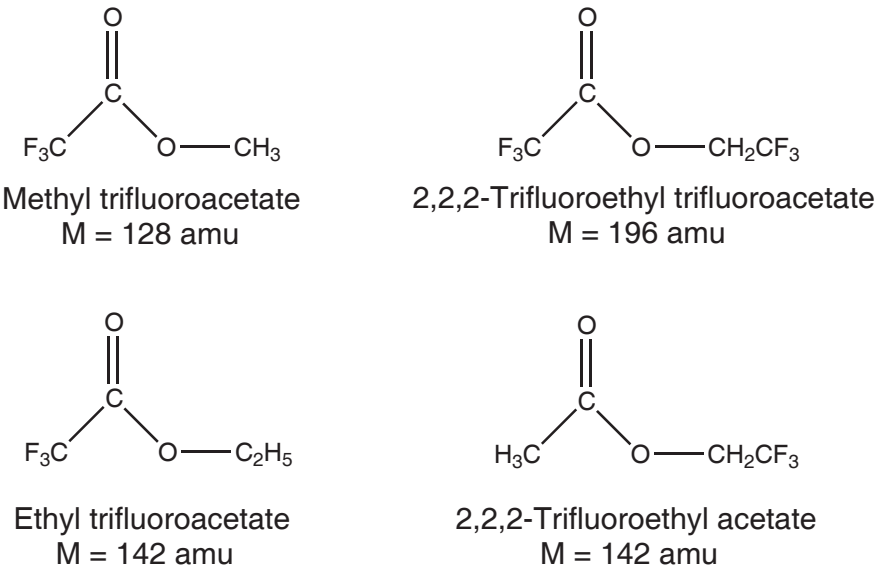

Figure 4.25: Molecular structure of the four investigated esters.

The influence of the length of the introduced hydrocarbon chain as well as the effect of fluorination of the ester chain can be studied. A comparison of the reactivity of the constitutional isomers ethyl trifluoroacetate and 2,2,2-trifluoroethyl acetate provides some information on the influence of the position of the CF_3 group on the fragmentation pattern.

4.3.1 Formation of the carboxylate anion in isolated ester molecules

Electron attachment experiments to different ester molecules show product formation mainly via low energy features (high energy contributions are also present). According to the discussion of resonances in Chapter 2 the low energy resonances ($\approx$0–3 eV) are assigned to single particle shape resonances while those at higher energy can be considered as core excited resonances.

Production of the carboxylate anion

For dissociative electron attachment to isolated molecules of the four different esters some common tendencies in reactivity are found. In contrast to the results obtained for methylated thymine the introduction of a hydrocarbon chain R does

not block the bond rupture at this specific position in the esters. The closed-shell anions CF_3COO^- for the trifluoroacetic acid esters and CH_3COO^- for the fluorinated acetic acid ester are formed with considerable intensity (see Fig. 4.26) via the following reaction scheme.

$$CF_3COOR + e^- \longrightarrow CF_3COOR^{-\#} \longrightarrow CF_3COO^- + R, \quad R = -CH_3, -C_2H_5, -CH_2CF_3 \tag{4.25}$$

$$CH_3COOR + e^- \longrightarrow CH_3COOR^{-\#} \longrightarrow CH_3COO^- + R \tag{4.26}$$

As shown in Fig. 4.26 the methyl and the ethyl ester of trifluoroacetic acid that are similar in structure form CF_3COO^- via a resonant process at about the same energy of ≈1ėV. Whereas this reaction is quite efficient in the methyl ester, the intensity of the detected anion decreases considerably regarding the ethylester. This can be due to a lower electron attachment cross-section of the molecule with a longer hydrocarbon ester group. For the ethyl ester additionally a second resonance leading to the formation of CF_3COO^- becomes visible in the spectrum with a peak maximum at 2.5 eV. The methyl ester shows contributions at higher energy around 11 eV.

The ion yield for the carboxylate anion from $CF_3COOCH_2CF_3$ shows a remarkable increase of the ion intensity and a considerable energy shift towards lower electron energy. In this case the formation of CF_3COO^- is already observed at energies around 0.1 eV. The introduction of an electron-withdrawing group in the ester chain weakens the O–C bond thereby facilitating the bond breaking at this position.

The thermodynamic threshold of the reactions can be calculated as follows.

$$E_{th} = D(C - O) - EA(CF_3COO) \tag{4.27}$$

Assuming 3.7 eV as the average binding energy of an O–C bond [7] and taking into account EA(CF_3COO)= 4.2 eV [56] the thermodynamic threshold becomes E_{th}= -0.5 eV, and thus the reaction is exothermic. The ion yield curve for the acetic acid ester shows that the corresponding resonance in this case is observed at higher energy with a maximum at ≈2.1 eV. Considering the lower electron

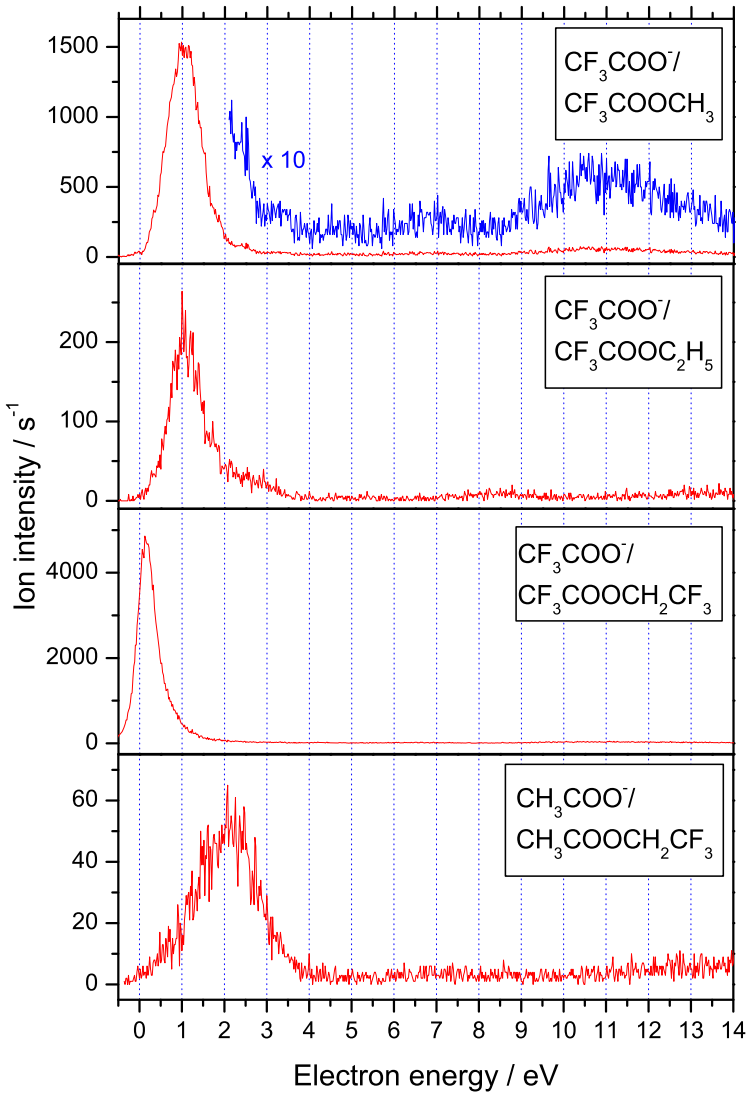

Figure 4.26: Spectra showing the ion yields for the carboxylate anions originating from the four different esters (for CF_3COOR with R =–CH_3 p =$4{\cdot}10^{-6}$ mbar, ΔE =200 meV; R =–C_2H_5 p =$2{\cdot}10^{-6}$ mbar, ΔE =200 meV; R =–CH_2CF_3 p =$2{\cdot}10^{-6}$ mbar, ΔE =150 meV; for $CH_3COOCH_2CF_3$ p =$1{\cdot}10^{-6}$ mbar, ΔE =240 meV).

affinity of CH_3COO (EA=3.39 eV) in comparison to CF_3COO the reaction becomes endothermic by ≈0.3 eV which is in good agreement with the observed

appearance energy. The comparatively low intensity of the ion signal is similar to previous results from DEA experiments with acetic acid where it was shown that the cross-section for the formation of the carboxylate anion is much lower than in case of trifluoroacetic acid [90].

From these results we can conclude that the efficiency of the carboxylate anion formation and also the electron energy to induce the corresponding resonant process is strongly dependent on the electronic nature of the introduced ester chain. Electron-withdrawing fluorine containing groups facilitate in case of $CF_3COOCH_2CF_3$ bond breaking and lower the necessary energy. The introduction of a pure carbohydrate shows an influence via the chain length.

Formation of CF_3^-

The fragmentation reaction leading to the formation of CF_3^- ions was also observed for all four different esters. The corresponding ion yields for this fragment are shown in Fig. 4.27.

$$\begin{aligned} CF_3COOR + e^- \longrightarrow CF_3COOR^{-\#} \longrightarrow CF_3^- + CO_2R, \\ R = -CH_3, -C_2H_5, -CH_2CF_3 \end{aligned} \tag{4.28}$$

$$CH_3COOR + e^- \longrightarrow CH_3COOR^{-\#} \longrightarrow CF_3^- + CH_3COOCH_2 \tag{4.29}$$

In all four different substances this anion is formed via at least two resonant states. While the low energy feature is at similar energies as the resonances that lead to the formation of the carboxylate anions there is a second resonance present at higher energy. The strongest CF_3^- signal is observed from trifluoroacetic acid methylester with peak maxima of 1.5 and 7.2 eV and a weak contribution at higher energy around 10–11 eV. The resonances for the ethyl ester seem to be shifted to lower energy in comparison to the methyl ester. From 2,2,2-trifluoroethyl trifluoroacetate the CF_3^- is already observed at 0.5 eV and from a second resonance at about 6–7 eV. As for the formation of the carboxylate the resonances lie at considerably higher energies in case of the acetic acid ester with peak maxima of 3.2 and 9 eV.

The thermodynamic threshold for the CF_3^- loss is calculated in the same way as for the formation of the carboxylate anion. With the dissociation energy

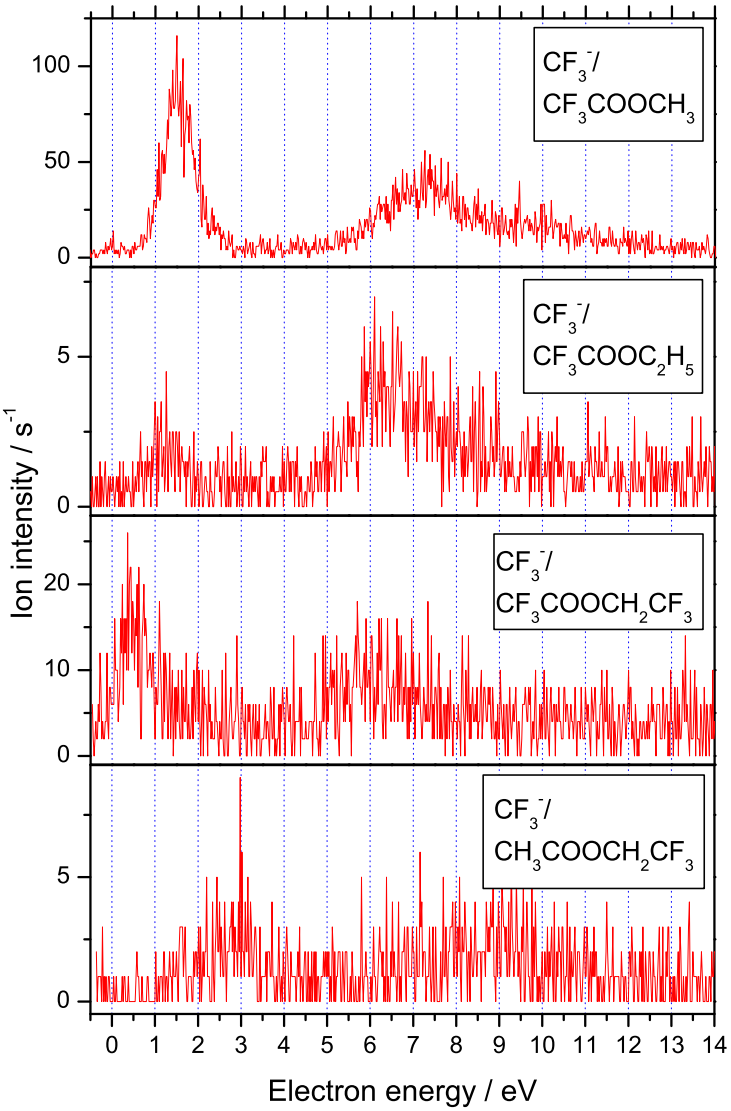

Figure 4.27: Spectra showing the ion yields for CF_3^- (for CF_3COOR with R =–CH_3 p=$4{\cdot}10^{-6}$ mbar, ΔE=200 meV; R=–C_2H_5 p=$2{\cdot}10^{-6}$ mbar, ΔE=180 meV; R=–CH_2CF_3 p=$8{\cdot}10^{-6}$ mbar, ΔE=160 meV; for $CH_3COOCH_2CF_3$ p=$1.3{\cdot}10^{-6}$ mbar, ΔE=240 meV).

D(C–CF_3)≈4.4 eV and the electron affinity EA(CF_3)≈1.8 eV the thermodynamic threshold of the trifluoroacetic acid esters becomes E_{th}≈2.6 eV. Although formally

in all four cases a C–C bond has to be cleaved, one has to take into account that the direct surrounding is different. Whereas for the methyl and the ethylester definitely the C–C bond next to the carbonyl group is cleaved, there are two possibilities for CF_3 loss in case of the fluorinated ethyl ester of trifluoroacetic acid. Bond cleavage can either occur next to the carbonyl group or in the ester chain. In the acetic acid ester the CF_3^- can only be abstracted from the ester group.

Abstraction of halocarbons

The methyl and ethyl ester of trifluoroacetic acid show an additional common reaction channel resulting in a fragment at M=94 amu which can be assigned to the anion CF_2COO^- (see Fig. 4.28).

$$\begin{aligned} CF_3COOR + e^- \longrightarrow CF_3COOR^{-\#} \longrightarrow CF_2COO^- + RF, \\ R = -CH_3, -C_2H_5 \end{aligned} \tag{4.30}$$

The formation of the same anion (by the abstraction of HF) was also observed in experiments with trifluoroacetic acid as already discussed in Chapter 4.2.3. [53, 50] As the energetic situation is similar for the esters, one can conclude that product formation is then driven by the formation of the respective halocarbons RF (methyl fluoride, ethyl fluoride). These halocarbons are as well as HF very stable molecules with a considerable binding energy of the newly formed C–F bond (D (F–CH_3) = 4.9 eV [108]). Hence the formation of these halocarbons can drive the reaction leading to CF_2COO^- by compensating the energy necessary to cleave the C–F bond in the precursor ion. The adiabatic electron affinity of CF_2COO^- was estimated in preliminary calculations at the B3LYP 6-31G(d) level to 3.2 eV [53].

The same product was also observed in ion cyclotron resonance experiments (ICR) following electron impact to methyl trifluoroacetate [111]. The authors propose a two step mechanism where first the fluoride-radical complex (as discussed in Chapter 4.2.3) is produced. Afterwards a subsequent nucleophilic substitution reaction at the methyl group takes place thereby forming the radical anion CF_2COO^- and the co-product R–F. The formation of F^- in these experiments took place in the energy range from 2.8–20 eV whereas in our experiments the

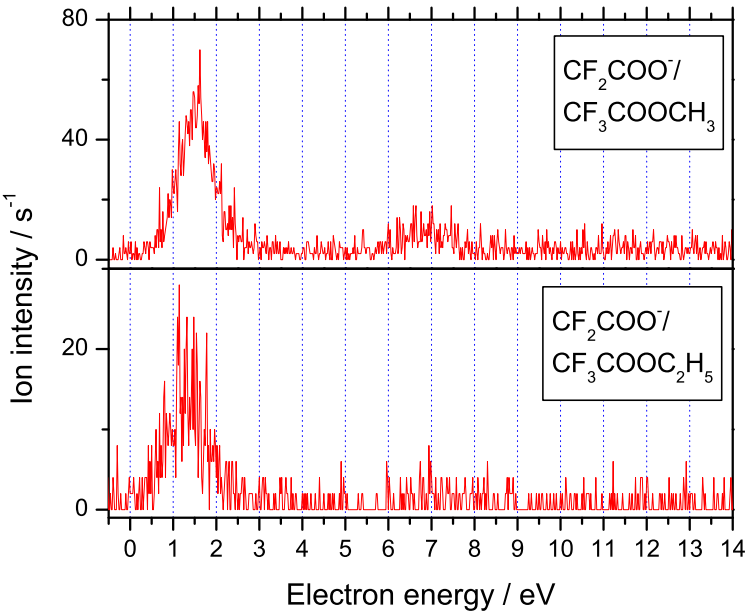

Figure 4.28: Spectra showing the ion yields for CF_2COO^- (for CF_3COOR with R=–CH_3, p=$4{\cdot}10^{-6}$ mbar, ΔE=200 meV; R=–C_2H_5, p=$2{\cdot}10^{-6}$ mbar, ΔE=200 meV).

CF_2COO^- anion is formed at considerably lower energy via a resonant process at ≈1.5 eV. The formation of F^- ions is not observed. This is in accordance with electron spin resonance experiments where no indication for F^--formation from $CF_3COOC_2H_5$ was observed [104]. Thus we conclude that the mechanism proposed by *Zhong et al.* is not likely in our case and that CF_2COO^- and the halocarbon may rather be formed in the excited precursor ion, e.g. in a cyclic transition state.

With these results we could demonstrate that CF_3COOCH_3 and $CF_3COOC_2H_5$ show a similar fragmentation following electron attachment. Both esters form the same products via resonances at similar energies, only the ion intensity is much weaker in case of the longer hydrocarbon chain. Due to the more extended degrees of freedom in this molecule, energy dissipation will suppress dissociation.

Common reaction channels in case of a fluorinated ester chain

The two esters containing a fluorinated ester group show further different fragments. As a common tendency the presence of fluorine in the ester chain makes the observation of the corresponding alkoxy anion $CF_3CH_2O^-$ possible (see Fig. 4.29). Whereas this reaction is quite efficient for the acetic acid ester and the

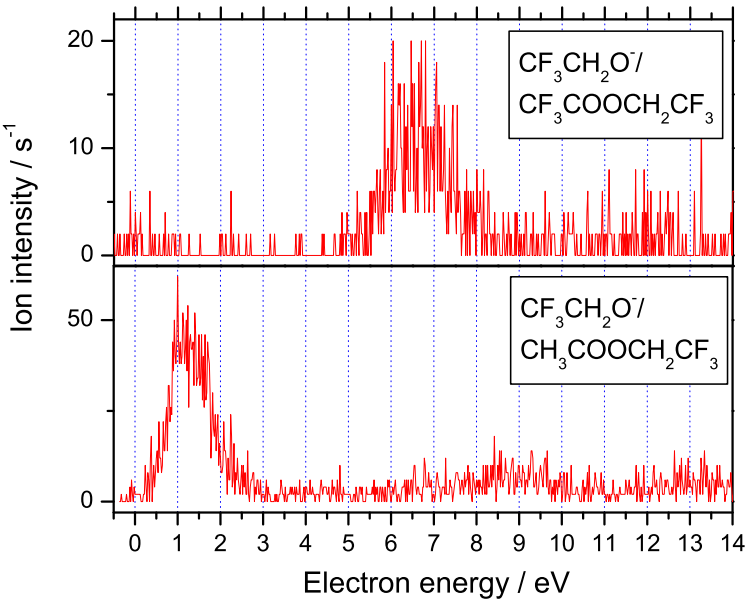

Figure 4.29: Spectra showing the ion yields for $CF_3CH_2O^-$ arinsing from DEA to $CF_3COOCH_2CF_3$ and $CH_3COOCH_2CF_3$ (for $CF_3COOCH_2CF_3$, p=$1{\cdot}10^{-6}$ mbar, ΔE=200 meV; for $CH_3COOCH_2CF_3$, p=$1{\cdot}10^{-6}$ mbar, ΔE=240 meV).

obtained ion yield is almost as high as for the formation of CH_3COO^- it is hardly observable for $CF_3COOCH_2CF_3$. In this case the signal could only be detected in studies with a very high electron current and a poor mass resolution. The formed alkoxy anion was already observed in the experiments with trifluoroethanol as a product of hydrogen loss as discussed in Chapter 4.1 [67]. There it was detected as the most intensive over all observed fragments. The comparison with ethanol shows that the corresponding alkoxy anion $CH_3CH_2O^-$ was formed only in weak

intensity. This difference in efficiency is in similarity with the observation that it is not formed from the methyl and ethyl ester of trifluoroacetic acid.

Hydrogen transfer in $CF_3COOCH_2CF_3$

Electron attachment to $CF_3COOCH_2CF_3$ additionally leads to the formation of a unique product within the investigated esters. With quite high intensity a fragment at M=114 amu was detected. Since the signal is about 15 % of $^{12}CF_3COO^-$ it cannot exclusively be explained by the presence of $^{13}CF_3COO^-$. For the corresponding ion yield spectra see Fig. 4.30. Hence we propose the formation of

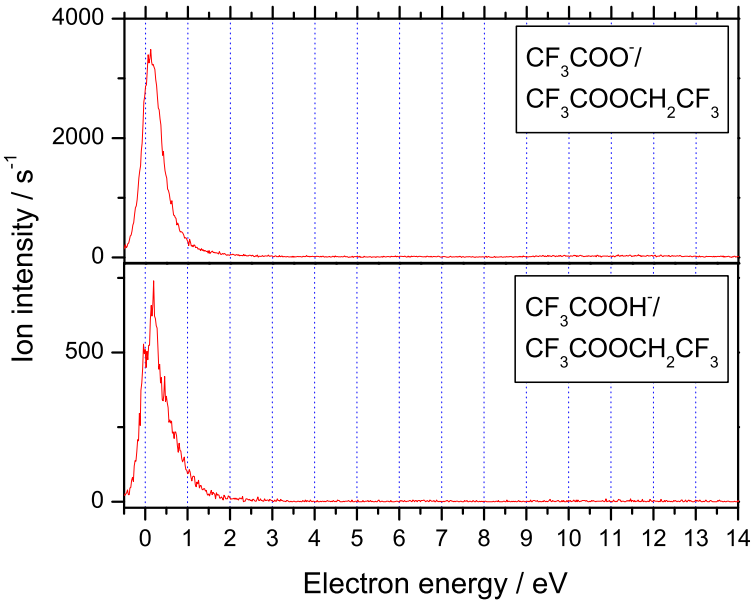

Figure 4.30: Spectra showing a comparison between the ion yields for the formation of the carboxylate anion and the production of the anion of trifluoroacetic acid from 2,2,2-trifluoroethyl trifluoroacetate (p=$2\cdot10^{-6}$ mbar, ΔE=150 meV).

the anion CF_3COOH^- by hydrogen transfer from the C–H position to the O–H position as depicted schematically in Fig.4.31. This process presumably becomes possible because of the introduction of a second electron-withdrawing groups in the ester chain. Therefore the C–H bond is weakened and formally a hydrogen

can be transferred to form the anion of trifluoroacetic acid CF_3COOH^-. This anion was already observed previously in experiments on molecular clusters of trifluoroacetic acid. There CF_3COOH^- was stabilized by evaporative electron attachment and hence the electron affinity of trifluoroacetic acid was considered to be positive [50]. The observation of the same anion in these experiments is a further indication of a positive electron affinity of CF_3COOH.

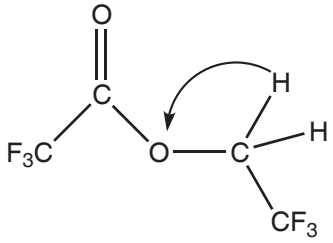

Figure 4.31: Schematic representation of hydrogen transfer in $CF_3COOCH_2CF_3$.

Loss of hydrogen

In case of the acetic acid ester $CH_3COOCH_2CF_3$ the additional fragment $(M-H)^-$ that is formed at low electron energy (≈1.5 eV) was detected, see Fig. 4.32. The comparable fragment was not observed in DEA to the trifluoroacetic acid

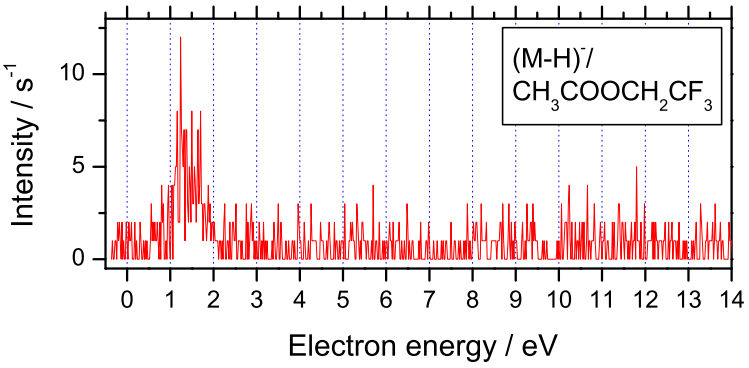

Figure 4.32: Spectra showing one further fragment arising from DEA to $CH_3COOCH_2CF_3$ (p=$1.3\cdot10^{-6}$ mbar, ΔE=240 meV).

esters. As already explained the loss of hydrogen is a ubiquitous process following electron attachment to organic molecules. Therefore it is surprising that it is not observed for the trifluoroacetic acid esters. To explain this difference in reactivity one has to consider the molecular structures of the investigated esters. For the esters of trifluoroacetic acid the only possible position for H-loss would be in the ester chain. In case of the acetic acid ester there is also the possibility that dehydrogenation occurs at the CH_3 group next to the carbonyl. Then an enolate anion can be formed that should be considerably more stable than the anion produced by the loss of hydrogen from the ester chain. This may explain why there is no dehydrogenation observable for the esters of trifluoroacetic acid. Thus we suggest that hydrogen loss from $CH_3COOCH_2CF_3$ more likely occurs at the CH_3-group in α-position.

4.3.2 Formation of halocarbons in clusters of trifluoroacetic acid esters

The same four different esters were also investigated with respect to changes in electron induced reactivity in molecular clusters in comparison with single molecules. A main interest in these experiments is to find out if the efficient formation of water observed in clusters of trifluoroacetic acid is still possible in the ester clusters or if a similar reaction can be detected. With these experiments information on the influence of quite strong intermolecular hydrogen bonds as in case of CF_3COOH, and the effect they have on the electron induced chemical reactions occurring in clusters can be investigated.

Similarly to the results obtained for single molecules in the gas phase there are some common tendencies in reactivity for molecular clusters of the different esters. For all esters the main fragments arising from DEA to single molecules were detected as well in the cluster experiment. These fragments can originate from DEA to molecules of the background, to single molecules traveling in the beam or from electron attachment to clusters.

Associative electron attachment to trifluoroacetic acid esters

Methyl trifluoroacetate and ethyl trifluoroacetate show again a similar reactivity. As observed frequently for electron attachment to molecular clusters the intact dimer and trimer anions were detected at electron energies close to 0 eV (see Fig. 4.33).

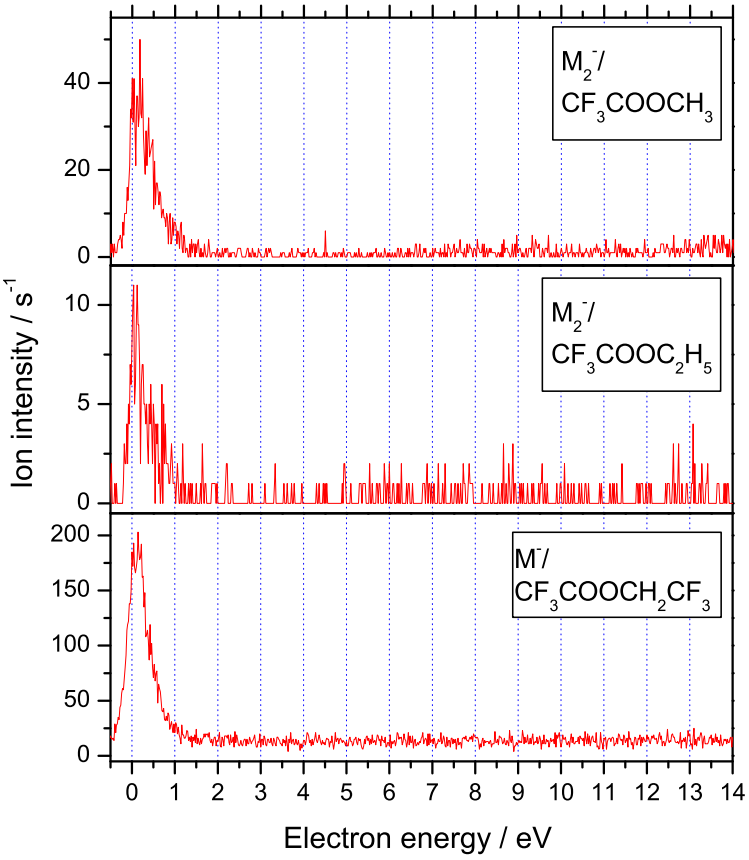

Figure 4.33: Spectra showing the intact dimer anions formed in clusters of methyl trifluoroacetate and ethyl trifluoroacetate and the molecular anion of $CF_3COOCH_2CF_3$. (Mixture 1:30 in Ar, p≈0.7 bar, ΔE≈200 meV for R = $-CH_3$, $-C_2H_5$; mixture 1:60 in Ar, p=0.5 bar, nozzle temperature -16 °C, ΔE≈250 meV for R = $-CH_2CF_3$)

The following reaction mechanism leads to product formation.

$$M_n + e^- \longrightarrow M_n^{-\#} \longrightarrow M_m^- + k\ M \tag{4.31}$$

For the 2,2,2-Trifluoroethyl trifluoroacetate the anionic intact molecule M^- was observed although the same product could not be detected in the experiments in the gas phase. Generally the formation of M^- proceeds via evaporative attachment as discussed for HCOOH and CF_3COOH. Higher homologues could not be detected in this case, but as the dimer already has a comparably high mass this can also be due to limitations in the detection efficiency of the used mass spectrometer in the corresponding mass range.

The observation of intact molecular anions with considerable intensity is similar to the results of CF_3COOH. Whereas the acid in the gas phase formed the stable carboxylate anion CF_3COO^- with the highest efficiency, the formation of the intact molecular anions in clusters was strongly favored, especially for higher order clusters although hydrogen loss was still observable but in weaker intensity. Thus a similar tendency for the acid and the esters is found. In contrary to the acid, in case of the esters neither the production of water in an intracluster reaction nor the formation of a product analogous to H_2O like R–O–R that remains attached to the carboxylate anions, is detected. For the esters of trifluoracetic acid the reactivity obviously changed towards another complex chemical reaction.

Complex chemical intracluster reactions

The esters of trifluoroacetic acid form following electron attachment a complex that can be either assigned to the formation of F^- which is solvated by an intact molecule of the corresponding ester or to the production of CF_3COO^- solvated by a newly formed molecule of the structure R–F (R = $-CH_3$, $-C_2H_5$, $-CH_2CF_3$). These complexes are formed at low electron energy with a maximum at E=0.3 eV (R = $-CH_3$, $-C_2H_5$) and E=0.1 eV (R= $-CH_2CF_3$) (see Fig. 4.34) via the following reaction mechanism:

$$M_n + e^- \longrightarrow M_n^{-\#} \longrightarrow CF_3COO^- \cdot RF + k\ M \tag{4.32}$$

The two proposed structures for the complex should be both possible considering thermodynamics. In case of $M{\cdot}F^-$ a C–F bond ($\approx$5.3 eV [108]) needs to be

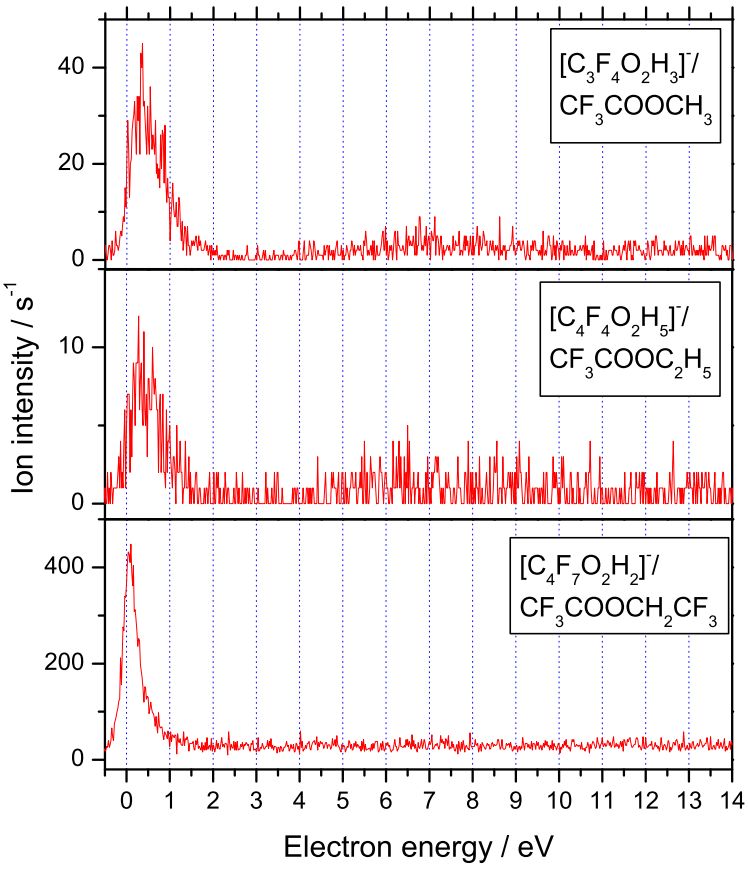

Figure 4.34: Spectra showing the anionic complexes $CF_3COO^-\cdot$ R–F / M·F^- formed in clusters of trifluoroacetic acid esters (Mixture 1:30 in Ar, p≈0.7 bar, ΔE≈200 meV for R = $-CH_3$, $-C_2H_5$; mixture 1:60 in Ar, p=0.5 bar, nozzle temperature -16 °C, ΔE≈250 meV for R = $-CH_2CF_3$).

cleaved, the EA of F (3.4 eV [1]) is gained and furthermore, the ionic interaction of F^- with the neutral molecule that is generally quite strong and can amount up to 2 eV for the example heaxfluoroacetone [55]. Although thermodynamically possible the proposed complex is unlikely to be formed as no formation of free F^- is observed.

The second possibility $CF_3COO^-\cdot$R–F consists of two structures already observed in the gas phase experiments. The anion CF_3COO^- is detected with

the highest intensity at low electron energies and the halocarbons R–F are co-products of the formation of the CF_2COO^- anion. The production of the CF_3COO^- anion is exothermic and to achieve the halocarbon a C–F bond in the target molecule is cleaved whereas a new C–F bond is formed in the halocarbon. Therefore the formation of this complex is possible at such low electron energies. As especially the formation of CF_3COO^- occurs with considerably high intensity the complex CF_3COO^-·R–F can be considered to be the more likely structure. Thus again an electron-induced intracluster chemical reaction takes place leading to the formation of a new neutral molecule that remains attached to the anionic fragment.

For R = $-CH_3$, $-C_2H_5$ also the complexes with one additional intact molecule were detected (CF_3COO^-·RF·M). The corresponding complex was not observed for R = $-CH_2CF_3$, but this can again be due to the comparable high mass of the proposed anionic complex and the limitations in detection of the used mass spectrometer in this mass range.

Formation of solvated CF_3^-

The methyl trifluoroacetate shows additionally the formation of a complex with the structure $CF_3^-\cdot$ M at an electron energy of 7–8 eV (see Fig. 4.35) that could not be detected for any of the other esters. The complexes are formed via the following reaction mechanism with m=1,2.

$$M_n + e^- \longrightarrow M_n^{-\#} \longrightarrow CF_3^- \cdot M_m + k\ M \tag{4.33}$$

There is no particular reason why it is not formed in case of the ethyl trifluoroacetate as these two molecules generally show a similar reaction pattern. Generally the ion intensities of the ethyl ester were considerably lower (as discussed above) so that it may be below the detection limit of our experiment.

Even more surprising is the fact that no experimental evidence of a solvated CF_3^- is found from 2,2,2-trifluoroethyl trifluoroacetate. The CF_3^- is formed in the cluster experiment with a much higher intensity than in the gas phase where it was hardly observable. This is not observed for other fragments and can thus not be explained by simply increasing electron scavenger properties of the molecular cluster as observed for HCOOH [60].

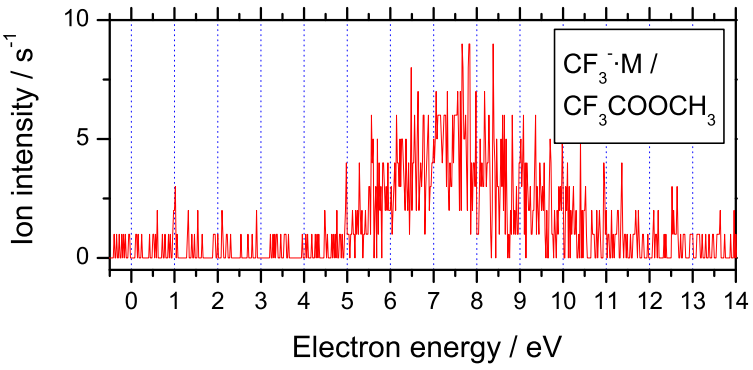

Figure 4.35: Ion yield showing the anionic complex CF_3^-·M formed in clusters of methyl trifluoroacetate (Mixture 1:30 in Ar, p≈0.7 bar, ΔE≈200 meV).

Production of the solvated acetate anion

In accordance with the results from the gas phase, electron interaction with clusters of $CH_3COOCH_2CF_3$ leads to the formation of anionic complexes that consist of the two main fragments from this experiment. While the acetate anion was detected as solvated complex with one or two neutral molecules attached ($CH_3COO^-{\cdot}M_n$) at an electron energy of ≈1–2 eV, the alkoxy anion was observed with only one neutral molecule attached ($CF_3CH_2O^-{\cdot}M$) from a low energy resonance about 0.7 eV and a broad feature at higher energy in the range 5–13 eV.

The following reaction mechanisms lead to the formation of the two different complexes.

$$\mathrm{M_n + e^- \longrightarrow M_n^{-\#}} \longrightarrow \mathrm{CH_3COO^- \cdot M_m + k\ M} \quad (4.34)$$

$$\longrightarrow \mathrm{CF_3CH_2O^- \cdot M_m + k\ M} \quad (4.35)$$

The corresponding ion yields are displayed in Fig. 4.36.

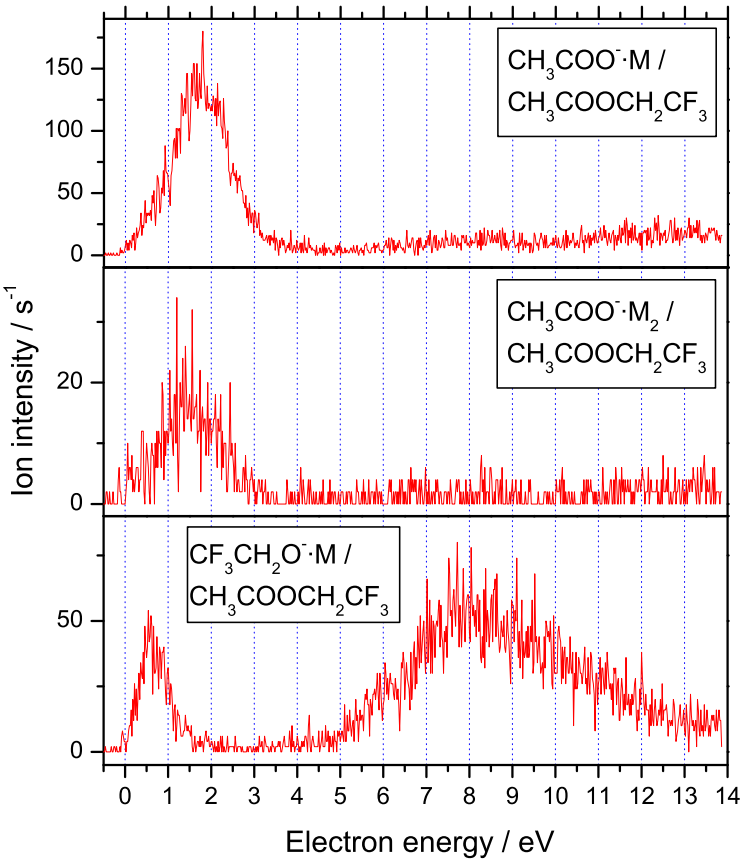

Figure 4.36: Spectra showing the anionic complexes $CH_3COO^-{\cdot}M_m$ and $CF_3CH_2O^-{\cdot}M$ formed in clusters of $CH_3COOCH_2CF_3$ (Mixture 1:30 in Ar, p=0.5 bar, ΔE$\approx$300 meV).

4.3.3 General conclusions for electron attachment to carboxylic acid esters

The experiments with different esters show that the introduction of a hydrocarbon group instead of hydrogen does not generally block bond rupture at this specific position. Furthermore, the electronic nature of the introduced ester chain has a particular influence of the electron induced reactivity as could be demonstrated on various examples.

Surprisingly, the abstraction of HF was not observed for the partly fluorinated ester compounds. In this case the formation of a halocarbon molecule is favored. The binding energy for the newly formed C–F-bond is also quite high but it is nevertheless lower than for an H–F-bond. Additionally, the abstraction of a halocarbon instead of hydrogen fluoride can be considered as another indication that the formed anionic product CF_2COO^- possesses a considerably high electron affinity that drives the corresponding reaction.

Further we could show that only the particular intermolecular interactions via comparably strong hydrogen bonds in trifluoroacetic acid as well as in formic acid clusters allow the formation of water in an intermolecular chemical reaction at the hydrogen bonding site. Instead of a reaction comparable to the formation of water a different complex reaction is observed for the esters leading to the formation of a halocarbon.

4.4 The investigation of ketones - electron attachment to acetones

The influence of different functional groups on electron induced reactivity can be further investigated by experiments with acetone, 1,1,1-trilfluoroacetone and hexafluoroacetone (see Fig. 4.37). The results for trifluoroacetone and hexafluoroacetone represent a further contribution in the series of molecules of the structure CF_3COR with different substituents R. The electron induced reactivity can thus be compared with the results for the corresponding acid and esters that were described above.

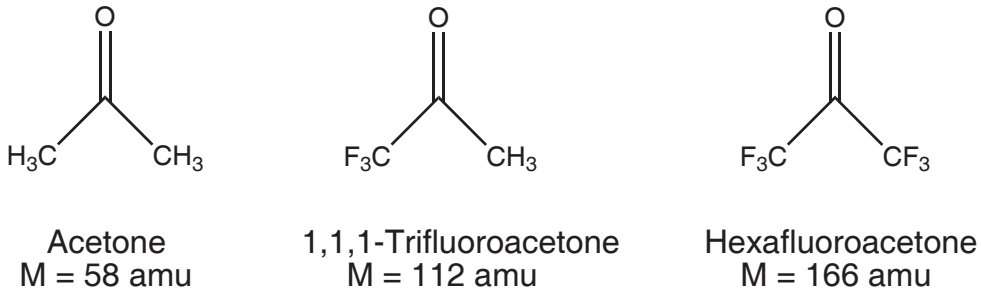

Figure 4.37: Molecular structures of the investigated molecules acetone, 1,1,1-trifluoroacetone and hexafluoroacetone.

By the investigation of the three acetone molecules the influence of the introduction of fluorine into hydrocarbon molecules can be studied in similarity to the esters as shown in the previous chapter. Thereby we go from the non-fluorinated acetone via the partly fluorinated 1,1,1-trifluoroacetone to the completely fluorinated hexafluoroacetone. A study on the corresponding isolated acetone molecules in the gas phase was already performed by *Oster* [69], the results of this study will be briefly summarized at the beginning of each section as they are the basis for the discussion of the cluster results.

4.4.1 The loss of hydrogen in clusters of acetone

The study of *Oster* [69] shows decomposition of acetone into five fragment anions following electron attachment. These fragments are dehydrogenated acetone $(M\text{-}H)^-$, $(M\text{-}H_2)^-$ formed by the abstraction of dihydrogen, $HCCO^-$ and OH^- formed

by multiple bond cleavage and also some rearrangement for the latter and O^- as a result of simple bond cleavage. The production of these fragments follows electron attachment mainly via a broad resonance in the energy range 7–12 eV that most likely consists of several overlapping non-resolved states. A time-of-flight study of the formed anions showed that they are all formed with thermal translational energy and thus the resonance was assigned to the core-excited resonance type. The observed signal intensities were for all anions relatively low. *Muftakhov and Fokin* additionally observed the fragment anions CH_3^- at an electron energy of 6.3 eV and H^- with a maximum in the ion yield at 8.8 eV with a shoulder around 6.8 eV [64]. They assigned the resonant state at 6.25 eV to the configuration $^2[n3s^2]$ as it correlates with the Rydberg state $^1[n3s^2]$ of the acetone molecule.

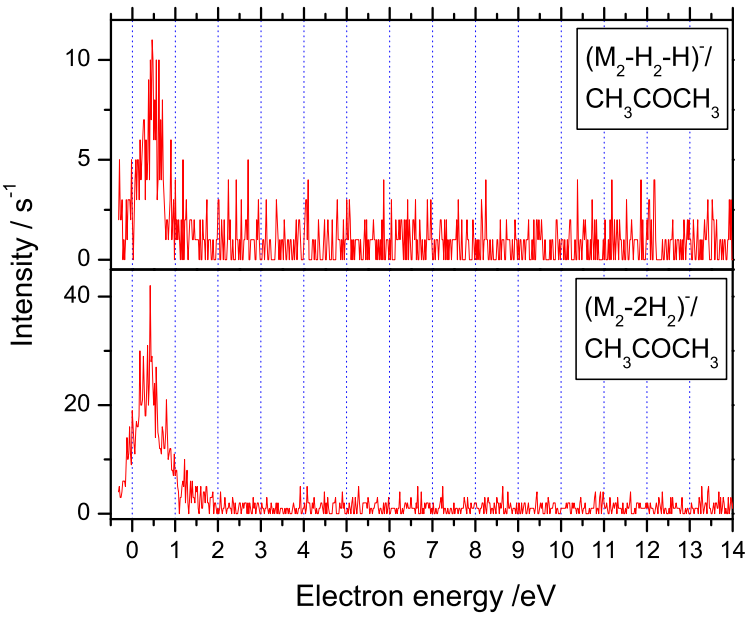

Figure 4.38: Spectra showing the anionic complexes arising from the loss of three or four hydrogen atoms from acetone (Mixture 1:20 in Ar, p=0.6 bar, $\Delta E \approx 500$ meV).

In the cluster experiments the ion intensities were as well very low, therefore the experiments were performed with a high electron current in favor of a better

electron energy resolution. The observed anionic complexes are a result of the loss of hydrogen and were observed in the compositions $(M_n\text{-}3H)^-$ and $(M_n\text{-}4H)^-$. Both complex configurations are formed via a low energy resonance with a maximum at ≈0.5 eV. The corresponding spectra are shown in Fig. 4.38.

For product formation three or four C–H-bonds need to be cleaved each of them with a binding energy D(H–CH_2COCH_3)=4.3 eV [108]. As the corresponding anionic complexes were observed from an energetic threshold at 0 eV the energy necessary for bond cleavage needs to be compensated by the electron affinity of the product and the formation of new bonds. A favorable reaction channel is the abstraction of molecular hydrogen H_2 with D(H–H)=4.5 eV [108] so that we propose the following reaction mechanisms.

$$M_n + e^- \longrightarrow M_n^{-\#} \longrightarrow (M_m - 3H)^- + H_2 + H + k\ M \quad n = m + k \quad (4.36)$$

$$\longrightarrow (M_m - 4H)^- + 2H_2 + k\ M \quad n = m + k \quad (4.37)$$

In case of both complexes there remains an energy of about 8 eV to overcome. One possibility would be that an intermolecular chemical reaction is taking place leading to cyclic products. Two possible structures for the two complexes, re-

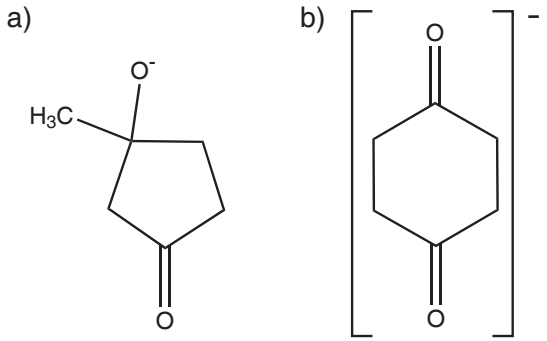

Figure 4.39: Two possible structures for the formed complexes in clusters of acetone: (a) $(M_2\text{-}3H)^-$ and (b) $(M_2\text{-}4H)^-$.

spectively are displayed in Fig. 4.39 both associated with the formation of two new C–C-bonds that is in a) leading to a five-membered ketone ring and in b) to a six-membered cyclic diketone structure of the hydrochinone type.

Taking into account an average binding energy for a C–C-bond of ≈3.5 eV an energy of about 1.5 eV remains that can most likely be covered by the electron

affinity of the formed complex. Thus the formation of a considerably stable cyclic structure is probable.

4.4.2 Formation of cyclic products in clusters of trifluoroacetone

For isolated molecules of trifluoroacetone *Oster* [69] observed a broad variety of fragment anions following electron attachment. Resonances around 4.5 and 8.5 eV mainly lead to product formation, but there are also resonances present around 0, 1, 9.5 and 12 eV for some specific anions. The resonance at 4.5 eV was assigned to electron capture into a π^*_{CO} orbital, that at 8.5 eV was attributed to a core-excited resonance. Due to simple bond cleavage *Oster* observed $(M\text{-}H)^-$, $(M\text{-}F)^-$, CF_3^-, F^- and O^-. Further fragments arising from multiple bond cleavage and/or rearrangement were an ion with the two possible structures $(M\text{-}F_2)^-$ or $(M\text{-}HF\text{-}H_2O)^-$, $HCCO^-$, OH^-, HF_2^- and C_2H^-. This fragmentation pattern could be approved in our measurements, the additional fragment CF_2^- was detected. The corresponding spectra are shown in the Annex C.1.

In the cluster experiments various anionic complexes were observed. In difference to the gas phase the detection of the intact molecular anions M_m^- (m=1–3) is then possible at an electron energy ≈0 eV (see Fig. 4.40). This is again due to evaporative electron attachment to molecular clusters as described earlier. The following reaction mechanism can be formulated.

$$(CF_3COCH_3)_n + e^- \longrightarrow (CF_3COCH_3)_m^- + k\ CF_3COCH_3 \quad (n = m + k) \quad (4.38)$$

Besides the associative electron attachment products there are as well complexes observable that are formed by dissociation. A fragment ion that was also observed in the gas phase is the dehydrogenated trifluoroacetone $(M\text{-}H)^-$ the structure of which will most likely be the considerably stable enolate anion.

$$(CF_3COCH_3)_n + e^- \longrightarrow CF_3COCH_2^- + H + k\ CF_3COCH_3 \quad (n = k + 1) \quad (4.39)$$

This anion may originate from electron attachment to clusters as well as to a single molecule traveling in the beam. The $(M\text{-}H)^-$ anions are mainly formed via resonances at higher energy in the broad range from 4 to 13 eV as shown in

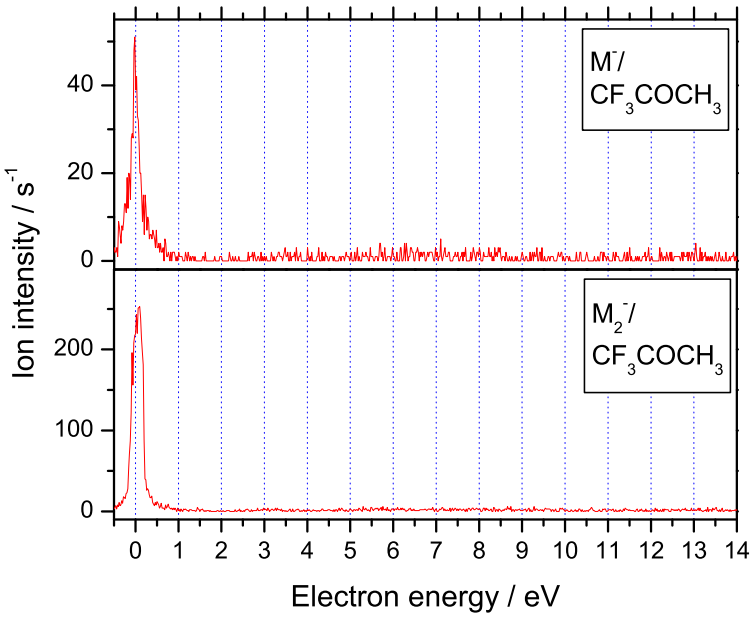

Figure 4.40: Ion yields showing the formation of the intact molecular anions M^- and M_2^- in clusters of 1,1,1-trifluoroacetone (Mixture 1:20 in Ar, p=0.1 bar, ΔE$\approx$200 meV).

Fig. 4.41. This non-resolved broad resonance most likely contains contributions of the two resonances observed for single molecules.

Furthermore, a complex $[C_3F_3H_4O]^-$ is detected mainly at an electron energy in the range of 5.5–9 eV and a small contribution around 0 eV.

$$(CF_3COCH_3)_n + e^- \longrightarrow [C_3F_3H_4O]^- + CF_3COCH_2 + k\ CF_3COCH_3 \qquad (n = k + 2) \tag{4.40}$$

Two likely structures can be proposed for this complex. One possibility would be the formation of the hydride ion solvated by an intact molecule of trifluoroacetone $H^-\cdot M$. In this case the thermodynamic threshold is calculated by taking into account the dissociation energy of the C–H-bond (4.3 eV [1]) and subtracting the

[1] As the binding energy for the C–H-bond in trifluoroaldehyde D(H–$COCF_3$) does not substantially differ from that in acetaldehyde D(H–$COCH_3$) [108], the binding energy for a C–H-bond in trifluoroacetone is estimated to be in the same range as that of acetone (see above).

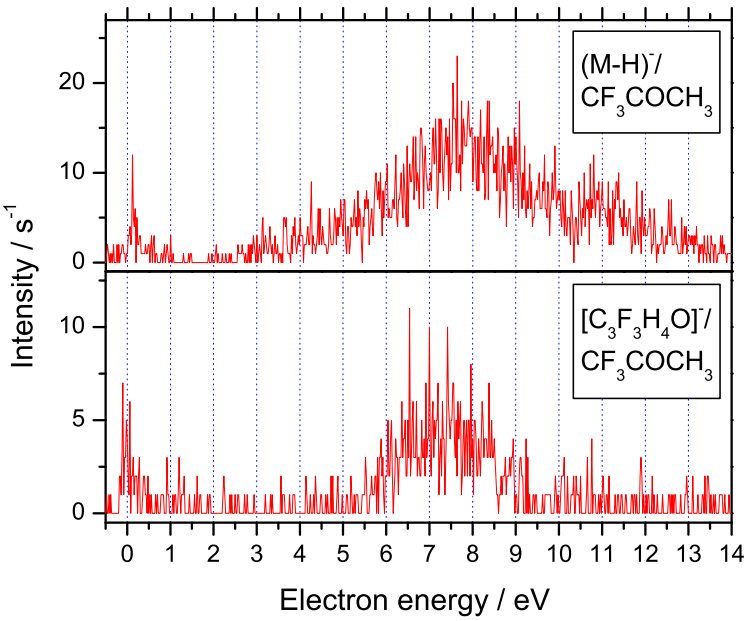

Figure 4.41: Ion yields showing the formation of the dehydrogenated trifluoroacetone anion $(M\text{-}H)^-$ and the complex $[C_3F_3H_4O]^-$ in clusters of 1,1,1-trifluoroacetone (Mixture 1:20 in Ar, p=0.1 bar, $\Delta E \approx 200$ meV).

electron affinity of the hydrogen radical (EA(H)=0.75 eV [1]). Thus one arrives at a threshold of 3.55 eV so that the formation of this complex should be possible from the high energy resonance but not from that around 0 eV.

A second possible structure for this anionic complex would be the dehydrogenated anion of trifluoroacetone solvated by molecular hydrogen. Considering thermodynamics this process is more favorable than the formation of $H^-\cdot M$. Taking into account the binding energy of a C–H-bond in trifluoroacetone D(C–H)=4.3 eV, the electron affinity of the trifluoroacetone enolat radical EA(F_3C–$COCH_2$)=2.65 eV [15] and the binding energy of molecular hydrogen D(H–H)= 4.5 eV [108] the thermodynamic threshold becomes 1.45 eV. Therefore the formation of this complex can also take place from the high energy resonance but it cannot explain the weak contribution around 0 eV.

In accordance with results for other molecules containing hydrogen and flu-

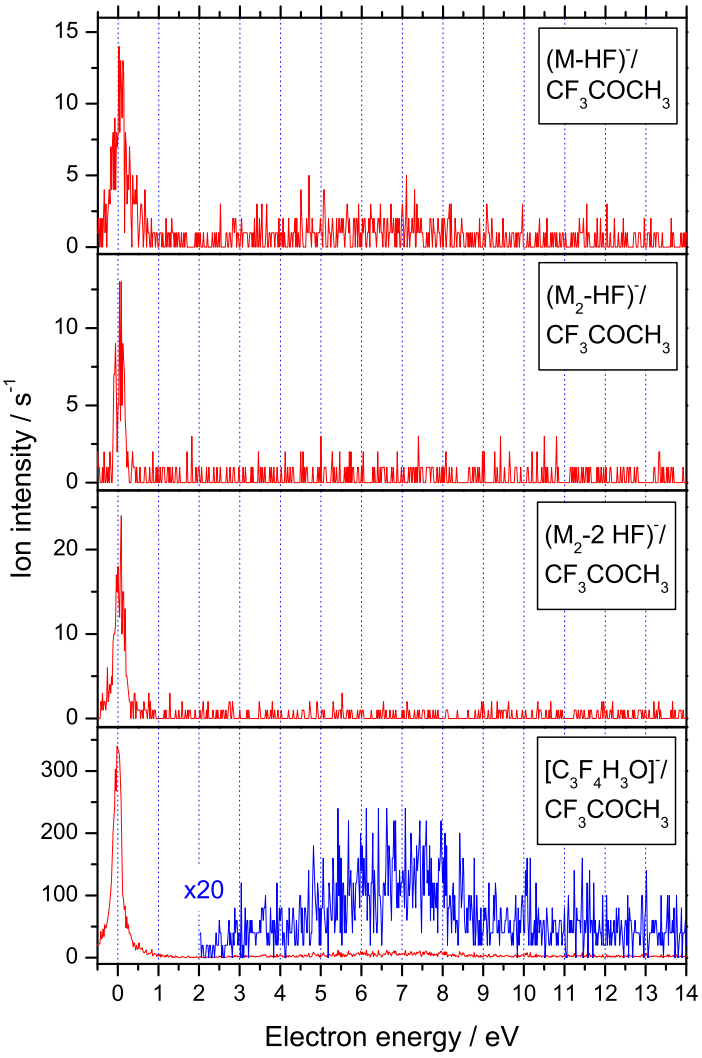

Figure 4.42: Ion yields showing the formation of various anionic complexes due to the abstraction of HF and on bottom a further complex arising from electron attachment to 1,1,1-trifluoroacetone with the composition $[C_3F_4H_3]^-$ (Mixture 1:20 in Ar, p=0.1 bar, ΔE$\approx$200 meV).

orine the abstraction of HF was also observed for trifluoroacetone. The corresponding spectra showing the formation of (M-HF)$^-$, (M_2-HF)$^-$ and (M_2-2HF)$^-$ around 0 eV are displayed in Fig. 4.42.

The fragment $(M\text{-}HF)^-$ is also observed following electron attachment to isolated molecules of trifluoroacetone. In this case it is the fragment detected with the highest intensity within all observed products. A calculation of the thermodynamic threshold plus the unknown electron affinity of $(M\text{-}HF)^-$ denoted as ΔH_0+EA(CF_2COCH_2) by taking into account D(C–H)=4.3 eV, the average binding energy of a C–F-bond D(C–F)=5.0 eV and the binding energy of HF D(H–F)= 5.9 eV [108] results in 3.4 eV so that one can assume that EA(CF_2COCH_2) is considerably high. The same anion was as well observed in the ion cyclotron resonance study of *Zhong et al.* [111]. They propose a two-step mechanism for product formation that was already discussed for CF_3COOH in Chapter 4.2.3.

Hydrogenfluoride is also abstracted from the dimer forming the complex $(M_2\text{-}HF)^-$. In this case HF can be either abstracted from one molecule thereby forming the same anion as in the gas phase which is then solvated by an intact molecule of trifluoroaceton or it can be abstracted from two different molecules in the cluster. If so two molecules can be linked by a new C–C-bond to form a hexane-2,5-dione compound (see Fig. 4.43) which is an energetically favorable process.

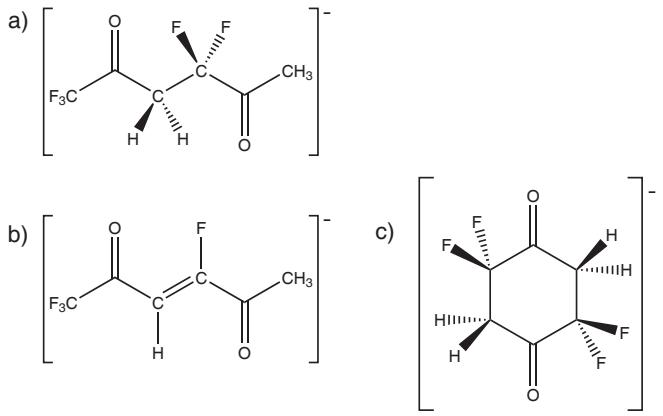

Figure 4.43: Possible structures for the complexes a) $(M_2\text{-}HF)^-$ b) and c) $(M_2\text{-}2HF)^-$.

Additionally, the abstraction of two molecules of HF from a dimer was observed. Here again the abstraction can occur only at one molecule and the newly formed anion would be solvated by an intact molecule. The possibility that is more favorable considering thermodynamics is the abstraction of HF from two different molecules of trifluoroacetone. Thereby again a chain-like structure, in

this case hexene-2,5-dion can be formed. Furthermore, one can also propose a cyclic structure of the hydrochinone type like for the abstraction of two molecules H_2 from a dimer of acetone (see above). The possible structures of the formed complexes are displayed in Fig. 4.43.

For the complex $[C_3F_4H_3O]^-$ also two possible molecular structures can be proposed. It is formed mainly via a resonance at 0 eV with a weak contribution at higher energy in the range 3–9 eV. One possibility would be the formation of $F^-{\cdot}M$. As the formation of F^- is also operative in the gas phase such a structure is likely. To form this complex, a C–F-bond with an average binding energy of D(C–F)=5.0 eV needs to be cleaved while the electron affinity of fluorine EA(F)=3.4 eV [1] is gained. Additionally, the binding energy between F^- and the intact molecule can be considerably high as demonstrated for hexafluoroacetone (≈2 eV) [55].

The second possible structure for this complex is the dehydrogenated anion of trifluoroacetone solvated by hydrogenfluoride $(M\text{-}H)^-{\cdot}HF$. As the abstraction of HF is a very efficient process in the gas phase such a structure is also likely. Considering thermodynamics of this process and taking into account the binding energies from above the energy that needs to be overcome by the ion-molecule binding energy in the complex becomes 1.25 eV. Thus both molecular structures seem to be possible and with the present experimental setup no further distinction can be obtained.

4.4.3 Self-scavenging processes in clusters of hexafluoroacetone

Electron attachment to hexafluoroacetone in the gas phase leads to the formation of anionic fragments by simple bond cleavage and also via associative attachment to the intact molecular anion $CF_3COCF_3^-$ [33, 65, 69]. *Oster* observed the fragment anions $CF_2COCF_3^-$, CF_3CO^-, CF_3^-, F^- and O^- via resonances at 3.7, 6.3, 8.5 and 10.5 eV. The resonance at 3.7 eV was attributed to electron capture into an unoccupied molecular orbital of π^*_{CO} character, while the higher energy resonances were assigned as core-excited resonances.

As further fragments *Harland and Thynne* detected the anions CF_2^-, CFO^- and $(CF_3)_2C^-$ [34]. The results of the gas phase studies performed in the framework of this work are presented in the Annex C.2 and they are in good agreement with the observations of *Oster*. As an additional fragment arising from electron attachment to single molecules of hexafluoroacetone we could detect an anion which was formed by the abstraction of F_2O at an electron energy around 0 eV. For this anion the molecular structure $[FC{\equiv}CCH_3]^-$ can be proposed.

While M^- was formed in the gas phase exclusively via a narrow resonance around 0 eV there are also high energy contributions observable in clusters. A comparison with the spectra for another anionic complex ($F^-{\cdot}M$) formed in the cluster as displayed in Fig. 4.44 shows that the high energy contributions for M^- formation have a similar resonance profile. The colored curves make it more clear that the broad feature observed at higher energy is most likely an overlap of at least three different resonant states (3.1, 5.5 and 7.1 eV).

Such processes leading to the formation of M^- in clusters at high energy while there are no high energy resonances observable in the gas phase are designated as self-scavenging processes (see Chapter 2.3). In a first step the electron is scattered in an inelastic or resonant inelastic way. The electrons are slowed down by the excitation of the molecule so that they can be attached to another molecule in the cluster via the low energy resonance. As in this case the resonant profile for M^- is matching with the one obtained for complexes formed by dissociation one can conclude that the scattered electrons mainly originate from autodetachment of a TNI.

$$\begin{aligned} M_n + e^-(\epsilon_1) &\longrightarrow M^{-\#} \cdot M_{n-1} \longrightarrow M^* \cdot M_{n-1} + e^-(\epsilon_2) \\ e^-(\epsilon_2) + M^* \cdot M'_{n-1} &\longrightarrow M'^{-\#} \cdot M_m^{(*)} + k\,M \longrightarrow M^- + k\,M^{(*)} \end{aligned} \tag{4.41}$$

Furthermore, the dimer anion M_2^- is detected that shows a similar resonance profile also with high energy contributions.

Complexes arising from dissociation are detected with the structure $F^-{\cdot}M_n$. These complexes were mainly detected for n=1, the composition n=2 is only detected in weak intensity. The resonance profile for $F^-{\cdot}M$ is indicating that the complex is formed via several partly overlapping resonances as discussed above. Additionally, a resonance with a maximum at 0.3 eV and weak contributions

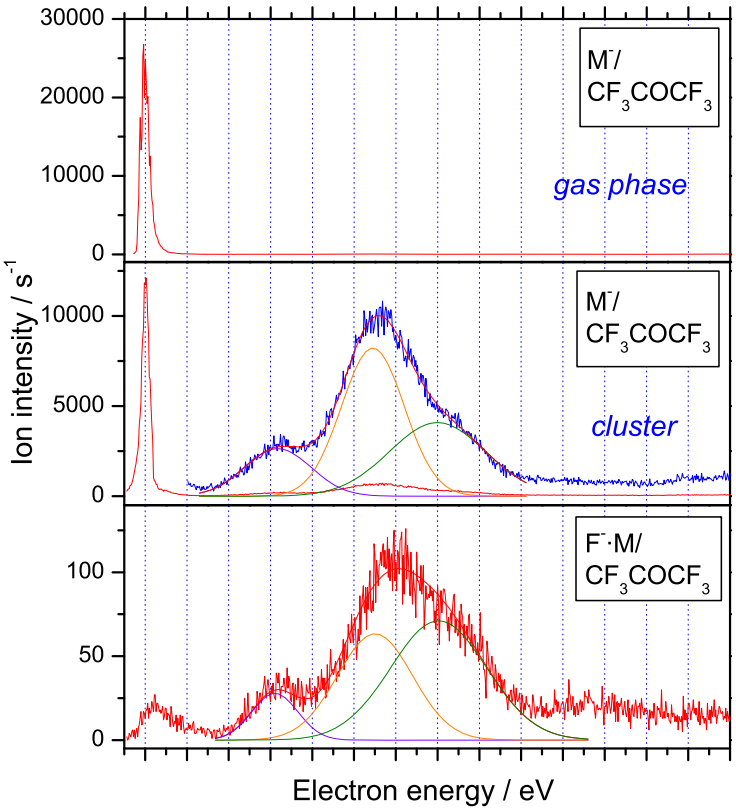

Figure 4.44: Ion yield curves showing the formation of M^- in electron attachment experiments to gas phase hexafluoroacetone (top), the formation of M^- in molecular clusters of hexafluoroacetone (middle) and the production of an anionic complex $F^-{\cdot}M$ in hexafluoroacetone clusters (bottom). Gas phase: p=$5{\cdot}10^{-6}$ mbar, ΔE$\approx$210 meV; Clusters: Mixture 1:20 in Ar, p=1.75 bar, ΔE$\approx$250 meV.

around 10.7 eV are observable. The complexes are formed via the following reaction scheme.

$$M_n + e^- \longrightarrow M_n^{-\#} \longrightarrow F^- \cdot M + CF_2COCH_3 + k\,M \quad (n = m + k) \qquad (4.42)$$

Considering the thermodynamics for this reaction one has to take into account the average binding energy for a C–F-bond D(C–F)=5.0 eV, the electron affinity of the fluorine radical EA(F)=3.4 eV [1] and the binding energy of F^- to the

intact molecule that is about 2 eV [55]. Thus the reaction becomes exothermic by -0.4 eV.

4.4.4 General tendencies for electron attachment to acetones

The comparison of the different acetones shows that acetone and 1,1,1-trifluoroacetone have a common tendency to form cyclic or chain structures by the abstraction of the stable molecules H_2 or HF, respectively. A comparable reaction, the abstraction of F_2, is not observed for hexafluoroacetone. Taking into account the binding energies for the abstracted molecules ((D(H–H)=4.5 eV, D(H–F)=5.9 eV and D(F–F)=1.6 eV) it is obvious that F_2 is a considerably less stable compound and thus the abstraction of F_2 is energetically not as favorable as that of the other molecules. The electron induced reactivity then leads preferably to complexes of the structure $F^- \cdot M_n$.

The degree of fluorination influences the ability to stabilize the excess charge on the intact molecule. While an intact molecular anion is not detected for non-fluorinated acetone its formation is an efficient pathway for the perfluorinated acetone. The 1,1,1-trifluoroacetone can be considered as an intermediate between the non-fluorinated and the perfluorinated compound. For this molecule M^- is at least formed by evaporative electron attachment and thus indicating a positive electron affinity of the molecule.